

Dynamics of stochastic integrate-and-fire networks

Gabriel Koch Ocker*

*Department of Mathematics and Statistics
Boston University
Boston, MA 02215*

(Dated: February 17, 2022)

The neural dynamics generating sensory, motor, and cognitive functions are commonly understood through field theories for neural population activity. Classic neural field theories are derived from highly simplified, discrete state models of individual neurons. This calls into question their ability to describe the population dynamics of biophysical neural models. Here, we develop a general framework for studying mean field dynamics and fluctuation effects in integrate-and-fire networks. We construct the joint density functional for membrane potentials and spike trains in networks of integrate-and-fire neurons with stochastic spike emission. This reveals exact and approximate mean field theories for the activity in these networks. These mean field theories are simple neural activity equations with a new nonlinearity: a rate-dependent leak, which approximates the spike-driven resets of neurons' membrane potentials. We study the impact of spike resets on population dynamics, finding bistability between quiescent and active states in homogenous and excitatory-inhibitory pulse-coupled networks. In both cases, we compute the phase diagram for quiescent, active and bistable regimes in the coupling strengths and external input strength. We also find that fluctuations suppress activity in the active states. We then examine the relative roles of spike resets and recurrent inhibition in stabilizing network activity. A paradoxical reduction of inhibitory firing rates after stimulation is commonly understood to be a signature of an inhibitory-stabilized regime. Such paradoxical responses occur in wide regions of parameter space. Spike resets dynamically stabilize even excitatory-only networks, however, so that recurrent inhibition is not necessary to stabilize activity. Finally, we discuss perturbative and exact methods for examining fluctuations in these networks.

I. INTRODUCTION

The activity of neuronal populations underlies sensory, motor, and cognitive functions. Mathematical theories for predicting the macroscopic activity of neural populations are a core tool of computational neuroscience, psychology, and psychiatry [1–4]. These theories typically rely on neural mass equations, also called rate equations, activity equations or, if placed on a spatial domain, neural field equations:

$$\dot{v}_i = -v_i + \sum_j J_{ij} * \phi(v_j) + E_i, \quad (1)$$

where $*$ denotes a temporal convolution. These and similar equations are commonly understood as a coarse-grained model for the proportion of active neurons in a large population [5–9]. They are a mean field theory for populations of Markovian neurons that switch between active and quiescent states [10–13] or of generalized linear Poisson neurons (Eq. 7).

The true biophysics of neurons are, however, highly complex [14]. Neural field equations have been supplemented with some biophysical detail in an ad hoc fashion [3]. A principled mean field theory of more biophysical neuron models would expose how single-neuron biophysics shape macroscopic population activity [15].

Integrate-and-fire models, which replace the nonlinear dynamics of spike generation by a simple fire-and-reset rule, are fruitful tools for investigating how network structure and synaptic and neuronal biophysics shape macroscopic activity [16, 17]. The classic mean field theory of integrate-and-fire networks focuses on the density of membrane potentials across a population [18]. If the net recurrent synaptic input current to each neuron is a white Gaussian process, the membrane potential density obeys a Fokker-Planck partial differential equation [19]. This allows the prediction of steady-state and weakly non-equilibrium population firing rates and pairwise statistics [20–24].

The assumption of white Gaussian input currents is, however, inconsistent with the resulting spike train statistics [25]. In some cases, the Fokker-Planck approach for the population voltage density can be extended to temporally structured fluctuations [26–28]. Alternatively, for generalized integrate-and-fire neurons with stochastic spike emission, population firing rates and pairwise statistics can be predicted from the density of interspike times rather than the density of membrane potentials [29–34]. Population density approaches expose approximate low-dimensional dynamics through eigenfunctions of the density evolution operator [35, 36]. The dimensionality of these approximations depends on the timescales present in the population density dynamics.

Here, we study the integrate-and-fire model with stochastic spike emission [29]. We construct the full joint probability density functional of a neuronal network's spike trains and membrane potentials using the response

* gkocker@bu.edu

variable path integral formalism [37–40]. This formalism is commonly applied to non-spiking models, e.g., [41–51]. It has also been applied to spiking models without nonlinear spike resets or in phase formulations that obscure them [52–56].

This construction exposes a new simple, deterministic mean field theory for stochastic integrate-and-fire networks: activity equations with an additional rate-dependent leak. This novel nonlinearity qualitatively shapes networks’ macroscopic dynamics. We study networks in an increasing order of complexity, progressing from uncoupled neurons to single-population recurrent networks and then networks with multiple cell types. We demonstrate bistable regimes in homogenous and excitatory-inhibitory networks. Comparing the deterministic mean field theory with an exact firing rate from renewal theory, we find that fluctuations suppress firing rates in the active state.

We then examine the relative roles of synaptic inhibition and spike resetting in stabilizing network dynamics. In the classic neural activity equations, inhibitory feedback is necessary to stabilize strong recurrent excitation [8, 57, 58]. In spiking neurons, however, the spike reset is sufficient to stabilize even strongly coupled excitatory networks. A paradoxical reduction of inhibitory activity after stimulation has been viewed as a signature of an inhibitory-stabilized regime [59–62]. We find paradoxical responses in wide regions of parameter space.

The path-integral construction also permits the diagrammatic calculation of arbitrary spike train statistics and exposes the coupling between different spike train statistics. For simple choices of the neurons’ voltage-rate function, these can be calculated fully analytically. This construction also exposes exact solutions for the equilibrium population firing rates and power spectra in large

networks via renewal theory [63]. We compare these with the result of perturbative expansions around equilibria of the mean field theory.

II. STOCHASTIC INTEGRATE-AND-FIRE MODEL

We introduce the stochastic leaky integrate-and-fire (LIF) model in discrete time first, before taking a continuous-time limit. At each small time step $t \in [T]$, neuron $i \in [N]$ generates $dn_{it} \in \{0, 1\}$ spikes. (n_{it} is the cumulative spike count of neuron i at time t .) Neuron i receives inputs $d\mathbf{n}$ through weighted synaptic filters \mathbf{J} . It also has a resting potential E_i , which may also depend on external applied currents. We take dn_{it} to be generated as a Bernoulli random variable η_{it} , with spike probability $f(v_{it})dt$, for some function $0 \leq f(v) \leq dt^{-1}$. If $f(v) = \theta(v - b)/dt$ where $\theta(x)$ is the Heaviside step function, the deterministic LIF neuron with threshold b is recovered [64]. In the continuous-time limit,

$$\dot{\mathbf{v}} = \frac{1}{\tau} (-\mathbf{v} + \mathbf{E} + \mathbf{J} * \dot{\mathbf{n}}) - \dot{\mathbf{n}}(\mathbf{v} - r). \quad (2)$$

Bold terms denote a vector or matrix-valued function. The last term models the spike reset. Rather than a spike decreasing the membrane potential by a fixed amount, we reset the membrane potential to within a negligible distance of the reset voltage r . This nonlinear coupling between the neuron’s spike train and membrane potential is the key feature of this model compared to classic generalized linear models [65]. We will non-dimensionalize the model, measuring time relative to τ and the membrane potential relative to r ($\tau \rightarrow 1, r \rightarrow 0$).

The joint density functional of the membrane potentials and spike trains, in the response variable path integral formalism, is (appendix A):

$$p[\mathbf{v}, \mathbf{n}] = \int \mathcal{D}\tilde{\mathbf{v}} \int \mathcal{D}\tilde{\mathbf{n}} \exp -S[\mathbf{v}(t), \mathbf{n}(t), \tilde{\mathbf{v}}(t), \tilde{\mathbf{n}}(t)], \quad (3)$$

$$S[\mathbf{v}, \mathbf{n}, \tilde{\mathbf{v}}, \tilde{\mathbf{n}}] = -\tilde{\mathbf{v}}^T (\dot{\mathbf{v}} + \mathbf{v} - \mathbf{E} - \mathbf{J} * \dot{\mathbf{n}} + \dot{\mathbf{n}}\mathbf{v}) + \tilde{\mathbf{n}}^T \dot{\mathbf{n}} - (\exp(\tilde{\mathbf{n}}) - 1)^T \mathbf{f}.$$

Here, $\mathbf{x}^T \mathbf{y} = \sum_i \int dt x_i(t)y_i(t)$ is the functional inner product, $*$ a matrix convolution, and $f_i(t) = f(v_i(t))$. The negative exponent, S , is the action functional. In the action, collecting terms first order in the response variables $\tilde{\mathbf{n}}, \tilde{\mathbf{v}}$ exposes the N -dimensional deterministic mean field theory

$$\dot{\mathbf{v}} = -\mathbf{v}(\mathbf{1} + \mathbf{f}) + \mathbf{E} + \mathbf{J} * \mathbf{f}. \quad (4)$$

Here, the mean field value of \dot{n}_i is $f(v_i)$. To study fluctuations, we can expand around that mean field theory (appendix B). Compared to the classic activity equations, these dynamics differ in two ways. The first is the presence of the term $-v_i f(v_i)$. The second is the presence

of the non-saturating hazard function f , rather than the saturating sigmoid typically used in the classic activity equations, e.g., ϕ in Eq. 1 [5–8]. In the microscopic binary switching model, the sigmoid ϕ determines the single-neuron transition rates between active and quiescent states [11]. Here, f is the hazard function of the spiking neuron. It determines the instantaneous spike emission probability as a function of the membrane potential and should be a non-saturating function. In both cases, the nonlinearity is a property of individual neurons.

Can we map the new mean field theory, Eq. 4, onto the classic activity equations, Eq. 1, with an effective nonlin-

earity ϕ that includes the effect of this rate-dependent leak? Requiring $-\mathbf{v}\mathbf{I}\mathbf{f} + \mathbf{J}\mathbf{f} = \mathbf{J}\phi$, we find that if the coupling \mathbf{J} has a left inverse,

$$\phi(\mathbf{v}) = (\mathbf{I} - \mathbf{J}^{-1}\mathbf{v}\mathbf{I})\mathbf{f} \quad (5)$$

So to map the mean field theory of Eq. 4 onto the classic activity equations, the effective nonlinearity ϕ depends explicitly on the coupling \mathbf{J} ; it is no longer a single-neuron nonlinearity.

The other classic form of rate equation is $\tau\dot{v}_i = -v_i + \phi(\sum_j J_{ij} * v_j + E)$. This is also a mean field theory of binary switching neurons [10, 12]. To map Eq. 4 onto this would require $\phi((\mathbf{J} * \mathbf{v})_i + E_i) = -v_i - v_i f(v_i) + \sum_j J_{ij} * f(v_j) + E_i$. For particular choices of the coupling \mathbf{J} and nonlinearity f , such a function ϕ might exist. In general, mapping Eq. 4 onto this would require the nonlinearity to be $\phi(\mathbf{J}, \mathbf{v}, \mathbf{E})$ —a function of the coupling operator, activity variable, and baseline drive separately, rather than of just their sum. Mapping Eq. 4 onto the classic activity equations would thus introduce nonlinearities tailored to a specific LIF network, rather than specified as a modeling choice. This mapping is, however, not necessary; the mean field dynamics of Eq. 4 are amenable to direct

analysis.

III. IMPACT OF SPIKE RESET ON SINGLE-NEURON FIRING RATE

We first examine the input-rate transfer of a single neuron or, equivalently, an uncoupled population. The mean field firing rate, \bar{f} , is given by steady-state solutions of Eq. 4 with $\mathbf{J} = \mathbf{0}$. We first consider neurons with threshold-power law spike probability functions, $f(x) = [x - 1]_+^a$, which match the effective nonlinearity of mechanistic spiking models and biological neurons in fluctuation-driven regimes [66–70]. For a threshold-linear neuron with $f(v) = [v - 1]_+$,

$$\bar{f} = [\sqrt{E} - 1]_+. \quad (6)$$

The mean field theory for the stochastic LIF neuron predicts its equilibrium firing rate as a function of its membrane potential (Fig. 1b, dashed black line vs dots).

For comparison, consider a stochastic LIF model with a linear reset: each spike causes a decrease in the membrane potential of size r [29, 30, 71]. The action for that model is

$$S[\mathbf{v}, \mathbf{n}, \tilde{\mathbf{v}}, \tilde{\mathbf{n}}] = -\tilde{\mathbf{v}}^T (\dot{\mathbf{v}} + \mathbf{v} - \mathbf{E} - \mathbf{J} * \dot{\mathbf{n}} + \dot{\mathbf{n}}r) + \tilde{\mathbf{n}}^T \dot{\mathbf{n}} - (\exp(\tilde{\mathbf{n}}) - 1)^T \mathbf{f}. \quad (7)$$

with the N -dimensional mean field theory

$$\dot{\mathbf{v}} = -\mathbf{v} - \mathbf{f}r + \mathbf{E} + \mathbf{J} * \mathbf{f} \quad (8)$$

This has a similar form to the classic activity equation, Eq. 1, and can be directly mapped onto it with the substitution $J_{ii}(s) \rightarrow J_{ii}(s) - r\delta(s)$. For this reason, we say that Eq. 1 is a mean field theory for a stochastic LIF neuron with linear resets, also called a generalized linear model or 0th order spike response model [65]. The expansion around the deterministic mean field theory for the linear-reset model has the same form as that of the Poisson generalized linear model [53].

Without coupling, the mean field firing rate of the linear-reset model, with $r = v_{th} = 1$, is

$$\bar{f}_L = [(E - 1) / 2]_+ \quad (9)$$

For a peri-threshold stimulus, $E = \epsilon$ in Eq. 6, $\bar{f} = (\epsilon - 1)/2 + \mathcal{O}(\epsilon^2)$ and the two mean field theories match for infinitesimal firing rates. At finite rates, however, the linear-reset mean field theory provides a poor prediction for the stochastic LIF neuron (Fig. 1b, blue line vs dots).

At higher rates, Eq. 6 overpredicts the true firing rates (Fig. 1b, dashed black line vs dots). The expansion of the probability density functional around that mean field theory exposes systematic corrections to it (Appendix B). We can also calculate the rate exactly without recourse

to the fluctuation expansion. Due to the nonlinear reset mechanism, the spike train is a renewal process. With a constant drive E , the membrane potential evolves after a spike at time t as $v(t + s) = E(1 - \exp(-s))$, with $v(t) = 0$. The time-averaged firing rate is the inverse of the mean interspike interval. For threshold-linear f , the mean interspike interval is

$$\langle s \rangle = \ln \left(\frac{E}{E-1} \right) + \left(\frac{E}{e} \right)^{1-E} \gamma(E-1, E-1). \quad (10)$$

$\gamma(x, y)$ is the lower incomplete gamma function. The term $\ln \left(\frac{E}{E-1} \right)$ is the time for $v(t)$ to reach the threshold value of 1; the second term is the mean first spike time after that [63]. Comparing this to the approximate deterministic mean field rate, Eq. 6, we see that fluctuations suppress firing (Fig. 1b).

IV. MEAN FIELD THEORY OF HOMOGENOUS NETWORKS

Biological neural networks are coupled. We here study the simplest case: networks where the connectivity between neurons is homogenous. We take the synaptic weights between neurons from a distribution with negligible second- and higher-order cumulants. Furthermore,

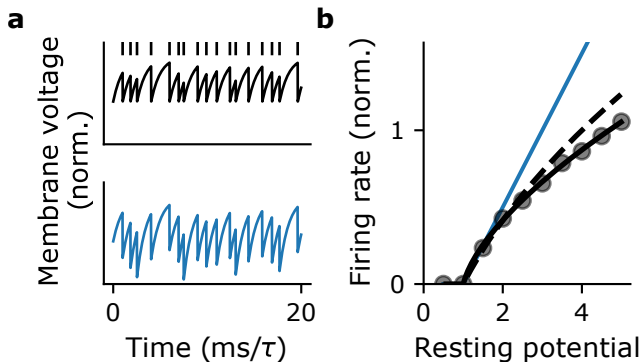


FIG. 1. **a)** Membrane potential traces of the stochastic LIF neuron (top, black) and a neuron with linear resets (bottom, blue). For comparison in this panel, the two neurons are forced to have the same spike times. **b)** Firing rate vs reversal potential, E , for the stochastic LIF neuron. Dots: simulation. Dashed black: mean field theory, $[\sqrt{E} - 1]_+$. Solid black: exact rate from Eq. 10. Solid blue: the mean field firing rate of the linear-reset model, $[(E - 1)/2]_+$.

we assume that the mean synaptic weight is $\mathcal{O}(1/N)$ so the total synaptic weight onto a neuron is $\mathcal{O}(1)$. An exemplar of this case is a network with weak ($J_{ij} \sim \mathcal{O}(1/N)$) but potentially dense (connection probability $\sim \mathcal{O}(1)$) connections [11]. To examine the interaction between synaptic connectivity, subthreshold dynamics, and stochastic spike emission in shaping network activity, we will average the partition function for the activity (equivalently, average the moment generating functional) over the synaptic connectivity (appendix C). In the limit of large N , this yields

$$Z^* = \int \mathcal{D}v \int \mathcal{D}\tilde{v} \int \mathcal{D}n \int \mathcal{D}\tilde{n} \exp \left(\tilde{v}^T (\dot{v} + v - E - J * \langle \dot{n} \rangle + \dot{n}v) - \tilde{n}^T \dot{n} + (e^{\tilde{n}} - 1)^T f \right). \quad (11)$$

The result is a single stochastic LIF neuron, receiving a self-consistent mean field input $J * \langle \dot{n} \rangle$. Robert & Touboul proved convergence to these mean field dynamics [72]. If the network is in an asynchronous state so $\langle \dot{n} \rangle$ is constant in time, after a spike at time t the membrane potential obeys

$$v(t + s) = (E + J \langle \dot{n} \rangle) (1 - \exp(-s)) \quad (12)$$

and the spike train is a renewal process. (We write J for the integral of the coupling kernel $J(s)$.) With a threshold-linear hazard function, the mean interspike interval is

$$\langle s \rangle = \ln \left(\frac{C}{C-1} \right) + \left(\frac{C}{e} \right)^{1-C} \gamma(C-1, C-1). \quad (13)$$

where $C = E + J \langle \dot{n} \rangle$.

To obtain a simple, fully deterministic approximation to this mean field theory, we can truncate the action of

the microscopic model, Eq. 3, at first order in \tilde{n} before averaging over the connectivity:

$$\dot{v} = -v - v f(v) + E + J * f(v). \quad (14)$$

This neglects all fluctuations, so we expect that it will not be quantitatively correct. Since the spike trains are conditionally Poisson, those fluctuations are driven by the expected intensity. We thus expect that Eq. 14 should be a good approximation when the true firing rate is low. As we will see below, it can provide a good qualitative description of the population dynamics, including bifurcations from quiescence.

V. BISTABLE ACTIVITY IN HOMOGENOUS NETWORKS

With a threshold-linear f , $f(v) = [v - 1]_+$, and pulse coupling, $J(s) = J\delta(s)$, there are three possible steady states of Eq. 14. The first is $v^* = E$, which exists if $E < 1$. There are two other possible steady states at $v > 1$,

$$v_{\pm}^* = \frac{J \pm \sqrt{J^2 + 4(E - J)}}{2} \quad (15)$$

which both exist if

$$E < 1 \text{ and } J > 2\sqrt{1 - E} + 2. \quad (16)$$

If $E > 1$, only v_+^* exists. If it exists, v_-^* (v_+^*) is unstable (stable). With $J > 2$ and $\frac{J(4-J)}{4} \leq E < 1$, both steady states exist and the firing rates are thus bistable, with v_-^* providing a separatrix between the attractors $v \rightarrow E$ and $v \rightarrow v_+^*$. The mean field theory has two saddle node bifurcation curves, where the unstable fixed point v_-^* meets either $v^* = E$ or v_+^* (Fig. 2a).

These bifurcations also appear in the underlying stochastic spiking model. We simulated a network of 100 stochastic LIF neurons (Eq. 2) with Erdős-Rényi connectivity ($p = 0.5$) with different values of the baseline drive E and coupling strength J (marked in Fig. 2a). At times 5 and 15, we applied pulse perturbations to the baseline drive and observed monostable or bistable behavior matching the prediction of the first-order mean field phase diagram (Fig. 2b-d).

The first-order mean field theory neglects all fluctuations in the spiking activity. Due to the nonlinear spike-voltage coupling imparted by the reset mechanism, those fluctuations can impact the firing rate. That coupling is described by loop corrections to the mean field firing rate. To determine the magnitude of all loop corrections, we computed bifurcation diagrams of the exact firing rate (Eq. 13; Fig. 2e, f). The first-order mean field theory systematically overestimates the true firing rates. This implies that fluctuations in the activity suppress firing.

In the model with linear resets and a threshold-linear hazard function, the mean field theory is linear in both

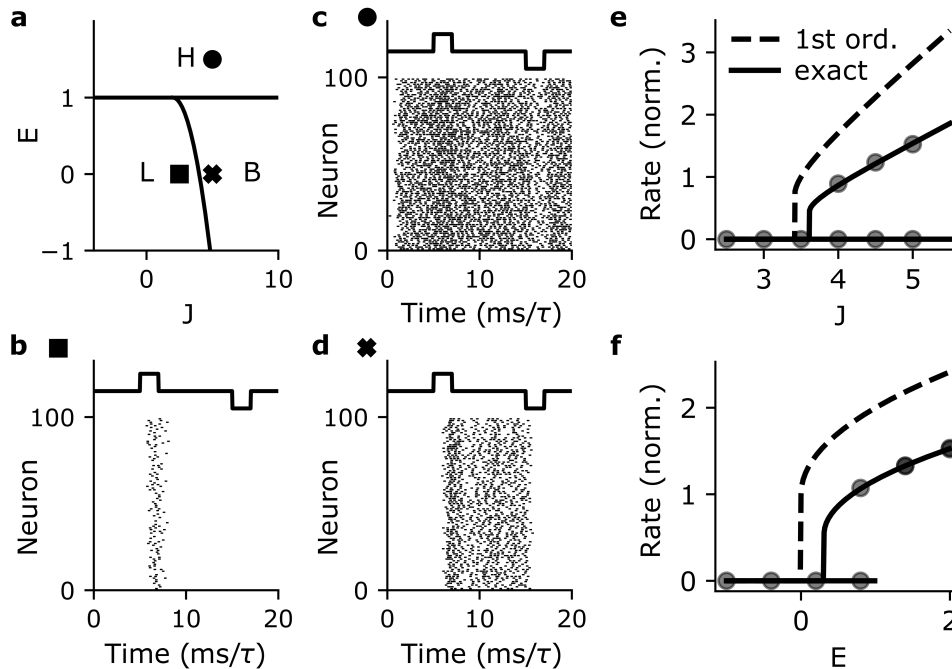


FIG. 2. Bistable activity in homogenous networks. **a)** Phase portrait of the first-order mean field theory, Eq. 14, in the input (E) vs coupling (J) plane. There are three possible states: low activity (L), high activity (H), and bistability (B). **b-d)** Raster plots of a homogenous networks activity at the parameter locations marked in panel a. At $t = 5$ and $t = 15$, perturbations of amplitude 2 and duration 2 are applied to the drive E (top). **e)** Bifurcation curve in J with $E = 1/2$. **f)** Bifurcation plot in E with $J = 4$. Grey circles: simulation. Black dashed: the first-order mean field theory of Eq. 14. Black solid: the exact rate of the disorder-averaged system, using a numerical self-consistent solution of Eq. 13.

the sub and suprathreshold regimes: $\dot{v}_L = -v - rf(v) + E + J * f(v)$. It thus cannot exhibit bistable activity. The bistability is due to the nonlinear coupling between the spiking and membrane potential.

The stochastic spiking network may not exhibit true bistability in the bistable regime of its deterministic mean field theory. Rather, the quiescent stable should be truly stable, while the active state is metastable. Fluctuations in the spiking activity may drive the network into the quiescent state. In the quiescent state, there are no fluctuations since all n -point correlation functions are sourced by the intensity $f(v)$, which we took to be 0 for $v < 1$. If the nonlinearity $f(v)$ were small but finite for $v < 0$, then fluctuations could be maintained in the quiescent state and both would be metastable. The slope of the hazard function at threshold can also play a key role in

metastability of the population activity [72].

VI. NETWORKS COMPOSED OF MULTIPLE CELL TYPES

Biological neural networks are composed of diverse types of neuron with cell type-specific connectivity, e.g., [73–80]. Motivated by this, we consider a network with M populations, which impose a block structure on the connectivity matrix \mathbf{J} . The average over the connectivity proceeds as for the single population, with an order parameter for each population's mean activity. This yields a M -dimensional mean field theory. The partition function is

$$Z^* = \int \mathcal{D}\mathbf{v} \int \mathcal{D}\tilde{\mathbf{v}} \int \mathcal{D}\mathbf{n} \int \mathcal{D}\tilde{\mathbf{n}} \exp \sum_{\alpha=1}^M \left(\tilde{v}_{\alpha}^T \left(\dot{v}_{\alpha} + v_{\alpha} - E_{\alpha} - \sum_{\beta=1}^M J_{\alpha\beta} * \langle \dot{n}_{\beta} \rangle + \dot{n}_{\alpha} v_{\alpha} \right) - \tilde{n}_{\alpha}^T \dot{n}_{\alpha} + (e^{\tilde{n}_{\alpha}} - 1)^T f(v_{\alpha}) \right). \quad (17)$$

The disorder-averaged spike train of population α ($\alpha \in [M]$) is an inhomogenous Poisson process. If the

population-averaged activities $\langle \dot{n}_{\beta} \rangle$ are constant in time,

the self-consistent mean first passage times are

$$\langle s_\alpha \rangle = \ln \left(\frac{C_\alpha}{C_\alpha - 1} \right) + \left(\frac{C_\alpha}{e} \right)^{1-C_\alpha} \gamma(C_\alpha - 1, C_\alpha - 1), \quad (18)$$

where $C_\alpha = E + \sum_{\beta=1}^M J_{\alpha\beta} \langle \hat{n}_\beta \rangle$. The first-order mean field approximation of the membrane potentials is

$$\dot{v}_\alpha = -v_\alpha - v_\alpha f(v_\alpha) + E_\alpha + \sum_{\beta} J_{\alpha\beta} * f(v_\beta). \quad (19)$$

VII. BISTABLE ACTIVITY IN EXCITATORY-INHIBITORY NETWORKS

Here, we consider the classic excitatory-inhibitory network with pulse coupling and mean connection strengths

$$\begin{pmatrix} J_{EE} & J_{EI} \\ J_{IE} & J_{II} \end{pmatrix} = \begin{pmatrix} J & -gJ \\ J & -gJ \end{pmatrix} \quad (20)$$

as in [20, 21] (Fig. 3a). With input E to both populations, the mean rates of the excitatory and inhibitory populations are equal since they receive the same external and recurrent inputs. The self-consistent fixed points, with positive rates, of Eq. 19 are at

$$v_\pm^* = \frac{J(1-g) \pm \sqrt{4E + J(g-1)(J(g-1) + 4)}}{2} \quad (21)$$

(Since the input and projections to each population are symmetric, their fixed point voltages are equal.) Both these fixed points exist if

$$\begin{aligned} E &< 1 \text{ and} \\ J &> 2 \left(1 + \sqrt{1-E} \right) \text{ and} \\ g &\leq 1 - 2 \left(\frac{1 + \sqrt{1-E}}{J} \right). \end{aligned} \quad (22)$$

If $E > 1$, only v_+^* exists. The Jacobian eigenvalue $J(1-g) - 2v$ is positive for the $-$ root and negative for the $+$ root. So if these fixed points exist, the one at higher v is stable and the other a saddle. With both population voltages under threshold, there is the stable fixed point $v^* = E$, if $E \leq 1$.

As for the single-population network, the existence conditions for these fixed points define saddle node bifurcation curves for the first-order mean field theory (Fig. 3b, c). If the inhibitory coupling strength is sufficiently low, we have the same bifurcation curves as in the single-population network (Fig. 3b). If the inhibitory coupling g is too strong, the only stable equilibrium is the low-rate state (Fig. 3c). For large J , the maximal g for bistability approaches 1 from below. If $g > 1$, the network with the same inputs to E and I populations cannot exhibit bistability.

These bifurcations also appear in the stochastic spiking network with block-Erdős-Rényi connectivity, $p_E =$

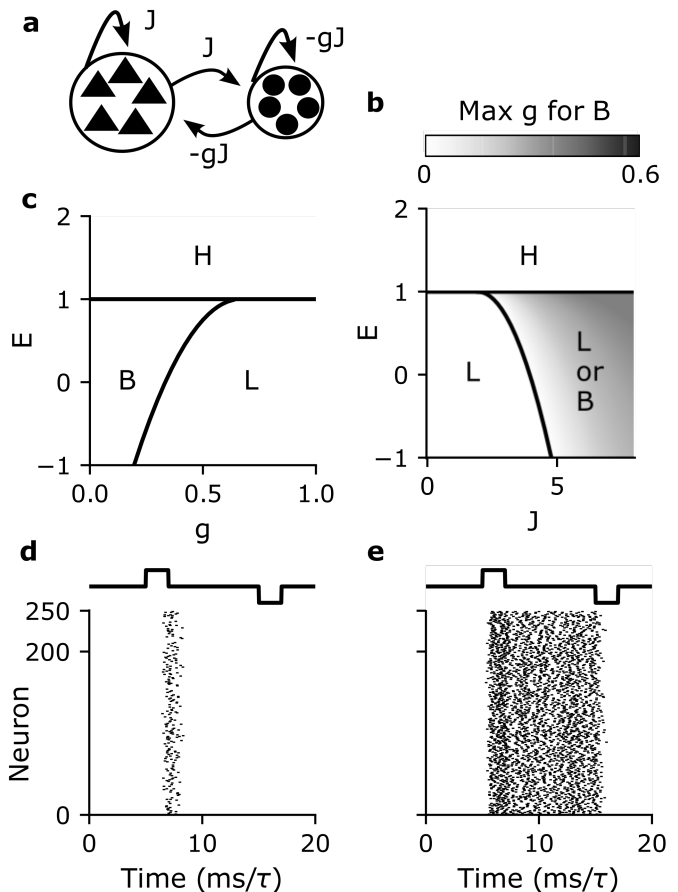


FIG. 3. Bistable activity in excitatory-inhibitory networks. **a)** Network diagram. **b)** Phase portrait of the two-dimensional first-order mean field theory, Eq. 19, in the input (E) vs coupling (J) plane. **c)** Phase portrait of the two-dimensional first-order mean field theory, Eq. 19, in the input (E) vs relative inhibitory strength (g) plane with $J = 6$. **d, e)** Example simulations with $(J, g) = (6, 0.3)$, with $E = -0.5$ (**d**) or $E = 0.5$ (**e**).

0.5 , $p_I = 0.8$, and mean connection strengths as in Eq. 20 (Fig. 3d, e). Similarly to the single-population network, the first-order mean field theory over-predicts the true firing rates so fluctuations suppress activity (Fig. 4).

VIII. INHIBITORY VS REFRACTORY STABILIZATION

In recent years, a body of work has emerged suggesting that mammalian cortex resides in an inhibitory-stabilized regime [8, 57, 59–62]. There are two requirements for an excitatory-inhibitory network to be inhibitory-stabilized: the network must occupy a stable fixed point for the activity, and the excitatory population would be unstable on its own. These are difficult to test experimentally. Fortunately, the inhibitory-stabilized regime has another signature: paradoxical responses to inhibitory neuron stimulation, which can take two forms. In an excitatory-

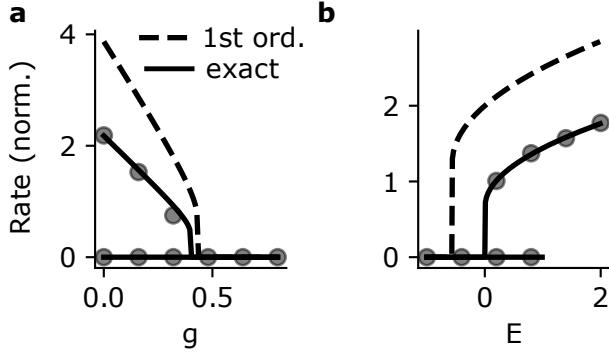


FIG. 4. Bifurcation diagrams of the excitatory-inhibitory network. **a)** Bifurcation diagram for the inhibitory strength g , with $(J, E) = (6, 0.5)$. Dots: simulation of a network with 200 **b)** Bifurcation diagram for the input strength E , with $(J, g) = (6, 0.25)$.

inhibitory network, stimulation of the inhibitory neurons leads to a reduction of their firing rates [58]. If there are multiple inhibitory subtypes, the net inhibitory input to pyramidal neurons decreases upon inhibitory neuron stimulation [81].

The inhibitory-stabilized regime, and paradoxical responses as its signature, are predictions of the classic activity equations of Eq. 1, which do not account for spike resetting of the membrane potential. Does an inhibitory-stabilized regime exist in the first-order mean field theory of Eq. 4? If so, in which parameter regions? Does it exhibit paradoxical responses to inhibitory stimulation?

These stability requirements are determined from the Jacobian matrix,

$$\begin{pmatrix} -1 - f_e^* + (J - v_e^*)f_e' & -gJf_i' \\ Jf_e' & -1 - f_i - (gJ + v_i^*)f_i' \end{pmatrix} \quad (23)$$

where $f_\alpha^* = f(v_\alpha^*)$ and $f' = f'_\alpha = f'(v_\alpha^*)$. Inhibitory stabilization requires that the first element of the Jacobian be positive (the excitatory-only subnetwork is unstable), but the maximum real part of its eigenvalues negative (the full network is stable). In the classic activity equations, the instability of exploding v is hidden by requiring the voltage-rate function ϕ to saturate [8, 58]. Saturated firing rates can thus be interpreted as a signature of the underlying instability in those networks, where ϕ is a modeling choice.

In the stochastic LIF model, saturation of f would imply that even for arbitrarily high membrane potentials, the spike probability in a finite time bin is bounded and the neuron cannot be guaranteed to spike. It is thus natural to take an unsaturated voltage-rate function f . For the threshold-linear hazard function, $f'(v_\alpha^*) = \theta(v_\alpha^* - 1)$, where $\theta(x)$ is the Heaviside step function. This leads to the requirement that for the excitatory network to be linearly unstable with a positive firing rate, $1 < v_E^* < J/2$. This is the same as the requirement that v_e^* be on the middle branch of the excitatory nullcline (Eq. 24).

The excitatory subnetwork is, however, guaranteed to have a stable fixed point (Eq. 15; Fig. 2). For any hazard function f that is smooth and increasing above threshold, we can easily rule out the simple instability of an exploding v in the excitatory subnetwork. Assuming that $v(t) \gg 1$, we expand f in its Taylor series around $v(t)$. If p is the leading exponent of that expansion, the leading-order term in $\dot{v}(t)$ is $-v^{p+1} < 0$. The mean field membrane potential dynamics are intrinsically stable due to the nonlinear spike reset dynamics. In contrast to the classic activity equations, this stability is not due to a modeling choice (ϕ) but is a consequence of the dynamics. Spike resets could thus be viewed as obviating the first requirement of an inhibitory-stabilized regime for networks of stochastic LIF neurons. While the excitatory subnetwork would be unstable at the fixed point of the full system, it does have a stable fixed point due to the intrinsic nonlinear dynamics of spike resetting.

When do paradoxical responses to inhibitory stimulation occur in the stochastic LIF network? To investigate this, we return to the tractable threshold-linear hazard function. We allow the external input to vary between the two populations, $\mathbf{E} = (E, hE)$ (Fig. 5a). h controls the relative strength of the input to the inhibitory population. When both population voltages are above threshold, the inhibitory and excitatory nullclines are at

$$v_i^* = \frac{-gJ + \sqrt{g^2J^2 + 4(J(v_e - 1 + g) + hE)}}{2} \quad (24)$$

$$v_e = (-(v_e^*)^2 + Jv_e^* + gJ - J + E) / gJ$$

h does not affect the excitatory nullcline but shifts the inhibitory nullcline. An increase in h will lead to a paradoxical reduction in firing rates if it shifts a stable fixed point to lower v_i^* . For example, consider the case when there is a single fixed point on the increasing side of the excitatory nullcline, to the left of its peak (Fig. 5b). Increasing h shifts the inhibitory nullcline up and to the left, moving that fixed point to a lower (v_e^*, v_i^*) . Depending on the magnitude of the shift, it may also take the dynamics through a bifurcation into a bistable regime. A sufficiently large increase in h can shift the network into a regime with no excitatory activity, which can also lead to a net decrease in inhibitory rates (Fig. 5b, c).

When does the system have a single fixed point with positive rates? The inhibitory nullcline is an increasing function of v_e . The excitatory nullcline increases for v_e close to 1 and decreases for sufficiently large v_e . So, at threshold ($v_e = 1$) the inhibitory nullcline must be below the excitatory nullcline:

$$\sqrt{(gJ)^2 + 4gJ + 4hE} < \frac{2}{gJ} (E + gJ - 1) + gJ. \quad (25)$$

If $h = 1$, this requirement imposes that $E > 1$; at $E = 1$ the two sides are equal, and the difference of the two sides grows as \sqrt{E} .

When is that fixed point on the increasing branch of the excitatory nullcline? The peak of the excitatory null-

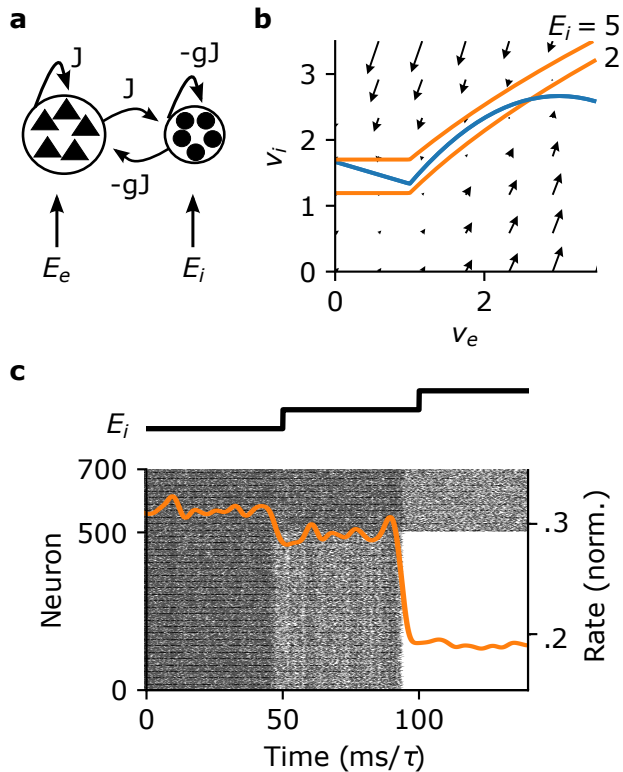


FIG. 5. Paradoxical responses to inhibitory stimulation. **a)** Excitatory-inhibitory network with asymmetric drive. **b)** Phase portrait and nullclines of the excitatory (blue) and inhibitory (orange) firing rates for the excitatory-inhibitory network with threshold-linear rate functions. **c)** Simulation of a block-Erdős-Rényi network with $p_{ee} = p_{ie} = 0.5$, $p_{ei} = p_{ii} = 0.8$. At time 0, $E_i = E_e = 2$. At times 50 and 100, E_i increases by 1.5. Orange: inhibitory population-averaged spike train, smoothed with a Gaussian kernel of width 2 for visualization. Parameters for **b**, **c**: $(J, g, E_e) = (6, 1/2, 2)$.

cline is at $v_e = J/2$. At the peak of the excitatory nullcline, $v_i = (-J^2/4 + J(1+g) + E)/gJ$. At $v_e = J/2$, the inhibitory nullcline should be above the excitatory nullcline:

$$\begin{aligned} & \sqrt{(gJ)^2 + 4gJ + 4hE + 2J(J-2)} \\ & > \frac{2}{gJ} \left(-\frac{J^2}{4} + J(1+g) + E \right) + gJ. \end{aligned} \quad (26)$$

Together, Eqs. 25 and 26 provide sufficient conditions for a paradoxical response to inhibitory stimulation in the first-order mean field theory. They predict a paradoxical response for sufficiently large J or g (Fig. 6a, c).

A paradoxical response could also occur from other dynamical regimes than the single fixed point on the decreasing branch of the excitatory nullcline, such as from a bistable regime. The first-order mean field theory also can quantitatively misestimate the average firing rates (figs. 2e, f; Fig. 4). To test whether the underlying spiking model exhibits paradoxical responses, we simu-

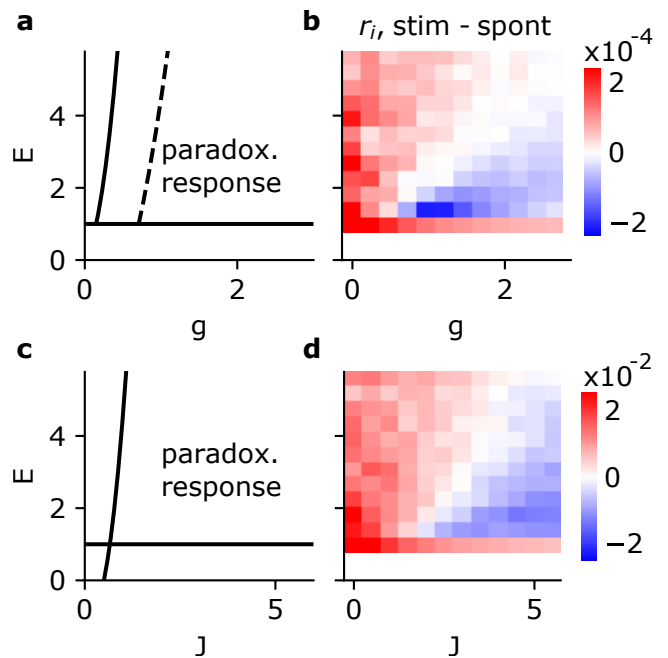


FIG. 6. Paradoxical responses to inhibitory stimulation. **a)** Boundaries of the single fixed-point paradoxical response region in the first-order mean field theory. Solid line: $(J, h) = (4, 1)$. Dashed: boundary for Eq. 26 with $(J, h) = (2, 1)$. The horizontal line at $E = 1$ arises from Eq. 25. **b)** Equilibrium response of the inhibitory population firing rate, in the stochastic spiking network (network as in Fig. 5c). Each simulation lasts for 200 time units; at time 100, the inhibitory drive switches from $E_i = E_e$ to $E_i = E_e + 0.1$. **c**, **d)** Similar to **a**, **b** but with $g = 2$.

lated excitatory-inhibitory networks while varying J and g . For each network, we applied a perturbation of amplitude 0.1 to the inhibitory population and computed the population-averaged firing rates before and after the perturbation. With J fixed and varying g , we observed paradoxical responses for sufficiently large g (Fig. 6b). Similarly, with g fixed and varying J , we observed paradoxical responses for sufficiently large J (Fig. 6d).

IX. FLUCTUATIONS

The deterministic mean field theory of Eq. 14 makes two major assumptions. First, it follows a saddle point approximation, accurate in the limit $N \rightarrow \infty$. That approximation admits a Gaussian finite-size correction by expanding the integrand to second order around the saddle point. We saw, however, that the mean field theory predicts the qualitative dynamics of relatively small populations. Second, Eq. 14 completely neglects fluctuations in the population activity due to spiking. The stochastic spike emission endows the population activity with cumulants of all orders, generated by the Poisson term of

Eq. 11. We saw earlier that these fluctuations suppress firing (Fig. 1b, Fig. 2e, f, Fig. 4). Spiking fluctuations can also play important roles in neural population codes [82] and models of long-term synaptic plasticity, e.g., [83–88].

The exact mean field theory, Eq. 11, is of an inhomogeneous Poisson process receiving a self-consistent mean input, $J\langle\dot{n}\rangle$, where $\langle\dot{n}\rangle$ is the population-averaged spike

$$p(s) = \begin{cases} 0, & s < \ln \frac{E+J\langle\dot{n}\rangle}{E+J\langle\dot{n}\rangle-1} \\ ((E+J\langle\dot{n}\rangle)(1-e^{-s})-1) \exp - \left((E+J\langle\dot{n}\rangle)e^{-s} + (E+J\langle\dot{n}\rangle-1) \left(s - 1 - \ln \frac{E+J\langle\dot{n}\rangle}{E+J\langle\dot{n}\rangle-1} \right) \right) \end{cases} \quad (27)$$

This provides an exact prediction for the interspike interval density, accurate even for populations of only a few hundred neurons (Fig. 7a). The interspike interval distribution defines the spike train power spectrum $C(\omega)$ of a renewal process [89]:

$$C(\omega) = \langle\dot{n}\rangle \frac{1 - |p(\omega)|^2}{|1 - p(\omega)|^2}. \quad (28)$$

Together, Eqs. 27 and 28 provide an exact prediction for the typical power spectrum in a large ($N \rightarrow \infty$) network. Computing the Fourier transform $p(\omega)$ numerically, we see that these predictions are quantitatively accurate even in simulations of a few hundred neurons (Fig. 7b, dots vs solid).

These renewal predictions rely on the Fourier transform of the interspike interval density, which may not be analytically tractable. Renewal theory also does not provide predictions for higher-order cumulants of the spike trains. As an alternative to the renewal theory, we construct a perturbative expansion for predicting arbitrary-order fluctuations by expanding v, \dot{n} around the deterministic mean field theory:

$$v(t) = \bar{v} + \delta v(t), \quad \dot{n}(t) = \bar{f} + \delta n(t) \quad (29)$$

where $\bar{f} = f(\bar{v})$, and \bar{v} is a solution of

$$\dot{v} = -v - v f(v) + E + J\langle\dot{n}\rangle \quad (30)$$

This yields the free and interacting actions, S_0 and S_V respectively:

$$\begin{aligned} S_0 &= -\tilde{v}^T (\delta_t + 1 + \bar{f}) \delta v - \tilde{v}^T \bar{v} \delta n + \tilde{n}^T \delta n - \tilde{n}^T f^{(1)} \delta v, \\ S_V &= -\tilde{v}^T \delta n \delta v - \sum_{p=2}^{\infty} \frac{\tilde{n}^p}{p!} \bar{f} - \sum_{\substack{p,q=1 \\ p+q>2}}^{\infty} \frac{\tilde{n}^p}{p!} \frac{f^{(q)}}{q!} (\delta v)^q. \end{aligned} \quad (31)$$

We now take \bar{v} to be an equilibrium of Eq. 30 with threshold-linear f ,

$$\bar{v} = \sqrt{J\langle\dot{n}\rangle + E} \quad (32)$$

train. After a spike, the membrane potential obeys Eq. 12, which defines the intensity $f(v(t))$. According to time-dependent renewal theory [89], the full interspike interval distribution is $p(s) = f(v(s)) \exp - \int_0^s dt f(v(t))$. For a threshold-linear hazard function $f(v) = [v - 1]_+$, the interspike interval distribution is

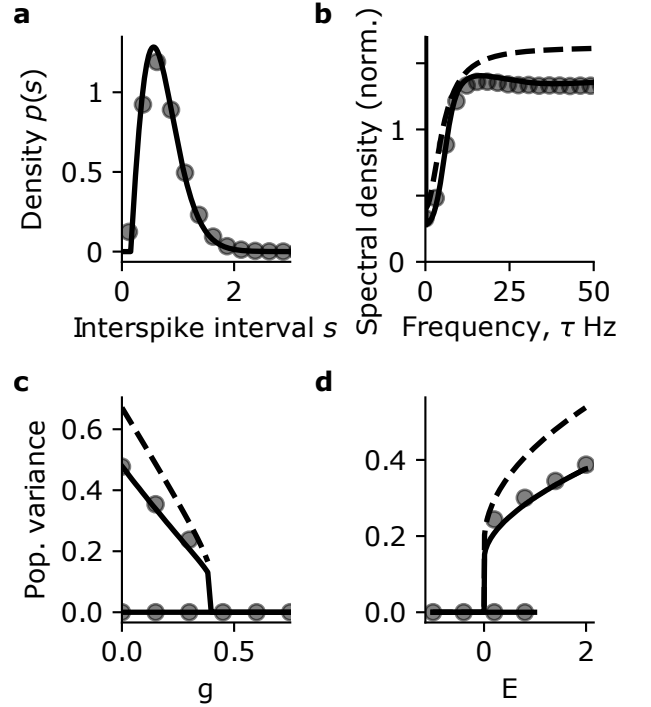


FIG. 7. Fluctuations in an excitatory-inhibitory network with symmetric external inputs, $E_e = E_i = E$. **a**) Interspike interval density with $(J, g, E) = (6, 0.3, 1.2)$. Dots: simulation of a network with 200 excitatory and 50 inhibitory neurons. Solid: the renewal prediction of Eq. 27. **b**) Power spectrum, parameters as in **a**. Solid: the renewal prediction of Eq. 28. Dashed: the tree-level approximation of Eq. 37. **c**) Bifurcation diagram for the inhibitory strength g , with $(J, E) = (6, 0.5)$. **d**) Bifurcation diagram for the input strength E , with $(J, g) = (6, 0.25)$.

Expanding around this,

$$\begin{aligned}
& \begin{pmatrix} \bar{\Delta}_{\delta n, \bar{n}} & \bar{\Delta}_{\delta v, \bar{n}} \\ \bar{\Delta}_{\delta n, \bar{v}} & \bar{\Delta}_{\delta v, \bar{v}} \end{pmatrix} (\omega) \\
&= \begin{pmatrix} 1 & -f^{(1)} \\ -\bar{v} & -i\omega - 1 - \bar{f} \end{pmatrix}^{-1} \\
&= \left(1 + \bar{f} + f^{(1)}\bar{v} + i\omega\right)^{-1} \begin{pmatrix} 1 + \bar{f} + i\omega & -f^{(1)} \\ -\bar{v} & -1 \end{pmatrix} \\
&= (2\bar{v} + i\omega)^{-1} \begin{pmatrix} 1 + \bar{f} + i\omega & -f^{(1)} \\ -\bar{v} & -1 \end{pmatrix}.
\end{aligned} \tag{33}$$

We used the threshold-linear hazard function f in the last line. Note that with a unit slope for f at \bar{v} , $f' = 1$ and the responses of v to spike and voltage perturbations are equal, $\bar{\Delta}_{v, \bar{n}} = \bar{\Delta}_{v, \bar{v}}$. We define the source vertex

$$\bar{f} = \bullet \tag{34}$$

and the (tree level/bare) propagators:

$$\begin{aligned}
\bar{\Delta}_{\delta n, \bar{n}} &= \text{---} \\
\bar{\Delta}_{\delta v, \bar{n}} &= \text{~~~~~} \\
\bar{\Delta}_{\delta n, \bar{v}} &= \text{~~~~~} \\
\bar{\Delta}_{\delta v, \bar{v}} &= \text{-----}
\end{aligned} \tag{35}$$

For example, the connected two-point function of the spike trains is then given by

$$\langle \delta n^2 \rangle = \text{---} + \text{---} + \dots \tag{36}$$

The expansion may contain terms sourced by n -point functions of all orders and diagrams with up to infinitely

many loops. The same is true for any cumulant of the activity. The tree-level approximation to $\langle \delta n^2 \rangle(\omega)$ is given by the first diagram in Eq. 36. For a single-population network,

$$\begin{aligned}
\langle \delta n^2 \rangle(\omega) &\approx f(\bar{v}) \bar{\Delta}_{\delta n, \bar{n}}(\omega) \bar{\Delta}_{\delta n, \bar{n}}(-\omega) \\
&= \left(\sqrt{J\langle \dot{n} \rangle + E} - 1\right) \frac{J\langle \dot{n} \rangle + E + \omega^2}{4(J\langle \dot{n} \rangle + E) + \omega^2}
\end{aligned} \tag{37}$$

For the E-I network with symmetric drives, $E_e = E_i$, this result holds with the replacement $J \leftarrow J(1 - g)$. At $\omega = 0$, this yields $\langle \delta n^2 \rangle(\omega) \approx f(\bar{v})/4$. In general, for a multi-population network the same type of approximation is given by its propagators $\bar{\Delta}_{\delta n, \bar{n}}$. Since we expanded around an equilibrium, we expect that if this tree-level approximation provides any good prediction, it should be at low frequencies; this is indeed the case (Fig. 7b, dashed vs dots). The $\omega \rightarrow \infty$ limit for the spectrum of a renewal process is its intensity. This perturbative expansion was around a stationary process with intensity $f(\bar{v}) = \sqrt{J + E\langle \dot{n} \rangle} - 1$, which is a deterministic approximation to the mean field population rate $\langle \dot{n} \rangle$, so we expect a mismatch between Eq. 37 and Eq. 28 at high frequencies.

The tree-level approximation of Eq. 37 neglects many contributions to the two-point correlation, such as the one-loop diagram in Eq. 36. This is one potential source of the quantitative error of Eq. 37 (Fig. 7b, dashed vs dots). Many of the diagrams contributing to the expansion of a connected correlation function, like Eq. 36, arise from the expansions of the propagators. Re-summing the expansions of the propagators would simplify that expansion considerably. That re-summing yields four coupled nonlinear integral equations. In the Fourier time domain, for linear f at \bar{v} ,

$$\begin{aligned}
\Delta_{\delta n, \bar{n}}(\omega) &= \bar{\Delta}_{\delta n, \bar{n}}(\omega) + \frac{f^{(1)}}{(2\pi)^2} \bar{\Delta}_{\delta n, \bar{v}}(\omega) \Delta_{\delta v, \bar{n}}(\omega) \int d\omega' \Delta_{\delta n, \bar{n}}(\omega') \Delta_{\delta v, \bar{n}}(\omega - \omega'), \\
\Delta_{\delta v, \bar{n}}(\omega) &= \bar{\Delta}_{\delta v, \bar{n}}(\omega) + \frac{f^{(1)}}{(2\pi)^2} \bar{\Delta}_{\delta v, \bar{v}}(\omega) \Delta_{\delta v, \bar{n}}(\omega) \int d\omega' \Delta_{\delta n, \bar{n}}(\omega') \Delta_{\delta v, \bar{n}}(\omega - \omega'), \\
\Delta_{\delta n, \bar{v}}(\omega) &= \bar{\Delta}_{\delta n, \bar{v}}(\omega) + \frac{f^{(1)}}{(2\pi)^2} \bar{\Delta}_{\delta n, \bar{v}}(\omega) \Delta_{\delta v, \bar{v}}(\omega) \int d\omega' \Delta_{\delta n, \bar{n}}(\omega') \Delta_{\delta v, \bar{n}}(\omega - \omega'), \\
\Delta_{\delta v, \bar{v}}(\omega) &= \bar{\Delta}_{\delta v, \bar{v}}(\omega) + \frac{f^{(1)}}{(2\pi)^2} \bar{\Delta}_{\delta v, \bar{v}}(\omega) \Delta_{\delta v, \bar{v}}(\omega) \int d\omega' \Delta_{\delta n, \bar{n}}(\omega') \Delta_{\delta v, \bar{n}}(\omega - \omega').
\end{aligned} \tag{38}$$

The dressed propagators $\Delta_{\delta n, \bar{n}}$, $\Delta_{\delta v, \bar{n}}$ are closed in each other and the bare propagators. Solving their two equations for the convolution term and setting the others equal reveals that $\Delta_{\delta n, \bar{n}}$ and $\Delta_{\delta v, \bar{n}}$ are linearly related

to each other at each ω :

$$\Delta_{\delta v, \bar{n}} = \frac{\bar{\Delta}_{\delta v, \bar{v}}}{\bar{\Delta}_{\delta n, \bar{v}}} (\Delta_{\delta n, \bar{n}} - \bar{\Delta}_{\delta n, \bar{n}}) + \bar{\Delta}_{\delta v, \bar{n}} \tag{39}$$

This provides a nonlinear integral equation for $\Delta_{\delta n, \bar{n}}$:

$$\begin{aligned} \Delta_{\delta n, \bar{n}}(\omega) = & \bar{\Delta}_{\delta n, \bar{n}}(\omega) + \frac{f^{(1)}}{(2\pi)^2} \bar{\Delta}_{\delta n, \bar{v}}(\omega) \left(\frac{\bar{\Delta}_{\delta v, \bar{v}}}{\bar{\Delta}_{\delta n, \bar{v}}} (\Delta_{\delta n, \bar{n}} - \bar{\Delta}_{\delta n, \bar{n}}) + \bar{\Delta}_{\delta v, \bar{n}} \right) (\omega) \\ & \times \int d\omega' \Delta_{\delta n, \bar{n}}(\omega') \left(\frac{\bar{\Delta}_{\delta v, \bar{v}}}{\bar{\Delta}_{\delta n, \bar{v}}} (\Delta_{\delta n, \bar{n}} - \bar{\Delta}_{\delta n, \bar{n}}) + \bar{\Delta}_{\delta v, \bar{v}} \right) (\omega - \omega') \end{aligned} \quad (40)$$

We solve this by fixed-point iteration from the initial condition $\bar{\Delta}_{\delta n, \bar{n}}$. The solution for $\Delta_{\delta n, \bar{n}}$ yields $\Delta_{\delta v, \bar{n}}$ from Eq. 39. We can then solve for $\Delta_{\delta v, \bar{v}}$ by fixed-point iteration. Those three yield the remaining full propagator, $\Delta_{\delta n, \bar{v}}$ (Fig. 8a). For the expansion around a steady state of the mean field theory, this re-summing has little effect on the propagators (Fig. 8b, c). We thus expect that the main source of error in the approximation of Eq. 37 arises from our expansion around an equilibrium of the mean field theory, rather than considering the nonequilibrium propagators [90].

DISCUSSION

We constructed a path integral representation for the joint probability density functional of the membrane potential and spike trains of a network of stochastic LIF neurons. This exposed a simple deterministic mean field theory for spiking networks: activity equations with an additional rate-dependent leak arising from the spike resetting (Eq. 4). Expanding $p[v, \dot{n}]$ around that N -dimensional mean field theory (appendix B) allows the study of fluctuations of and between identified neurons in a network of known connectivity. Large-scale electron microscopy (EM) is revealing such wiring diagrams, e.g., [91–103].

Here, we used the path integral representation to derive a population-averaged stochastic mean field theory for large networks with homogenous coupling, including multi-population systems like excitatory-inhibitory networks. We demonstrated bistability of the deterministic mean field theory and its extension to the stochastic system and studied the contributions of recurrent inhibition and spike resetting to stabilizing network activity. Excitatory-inhibitory networks of deterministic LIF neurons can also exhibit bistable equilibrium rates if the inhibition is not too strong [21]. The path integral approach exposes a purely deterministic mean field theory, similar in spirit to the classic neural activity equations [5–9]. This mean field theory exposed bistability through an elementary analysis of its equilibria. Robert & Touboul studied the homogenous stochastic LIF network rigorously [72]. They proved that the mean field process, Eq. 11, can have one or several invariant densities depending on the form of the firing function.

There are two complementary approaches to our focus on the density functional of sample paths, $p[v(t), \dot{n}(t)]$, for the stochastic LIF model. These complementary approaches focus on the time-dependent probability density function of the membrane potentials, $p(v, t)$, across

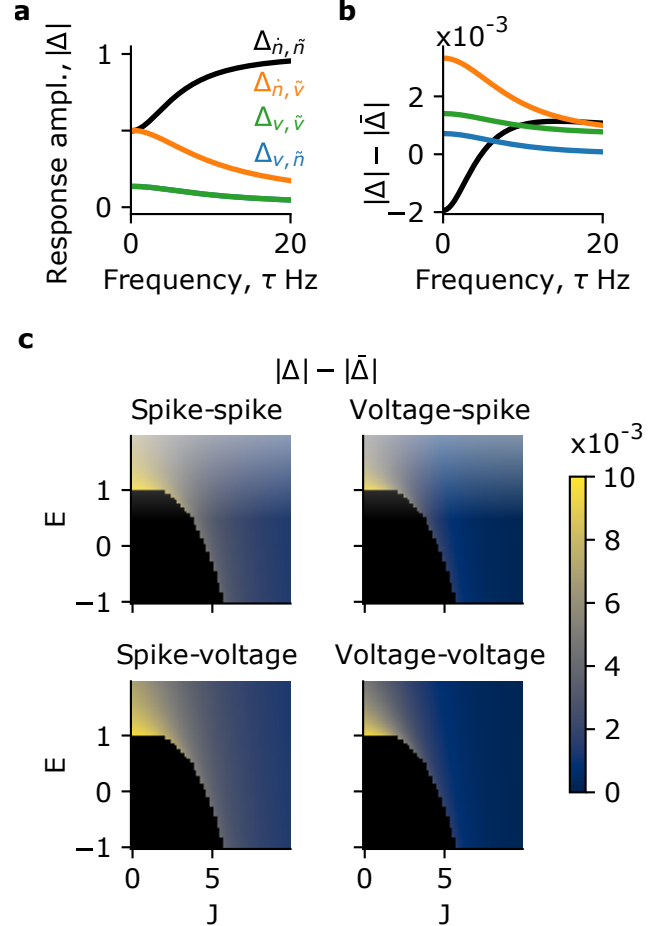


FIG. 8. Re-summed propagators. **a)** Re-summed propagators around the mean field equilibrium for a single-population network. Similarly to the tree-level propagators (Eq. 33), the voltage response is similar to a perturbation of the spikes or the voltage. **b)** Difference between the re-summed and tree-level propagators around the mean field equilibrium. In **a** and **b**, $(J, E) = (6, 0.5)$. **c)** Difference between the re-summed and tree-level propagators around the mean field equilibrium, at 0 frequency.

a population of neurons [18]. In the $N \rightarrow \infty$ limit and with $J_{ij} \sim 1/N$, the population density of membrane potentials in a stochastic LIF network obeys a Volterra integral equation [29, 30]. That integral equation can also be written as a partial differential equation, e.g., [104]. A finite-size correction introduces a stochastic term to the population density equations [34, 105]. These formulations rigorously expose the stochastic stability of the

population densities in a mean field limit [106–108].

The path integral approach is practical and flexible. It allows calculations of any joint cumulant of the spike trains and/or membrane potentials via diagrammatic methods [53], is amenable to finite-size corrections [52], and applies readily to other models, such as those with temporal synaptic interactions, spatially dependent connectivity, conductance-based or strong $\mathcal{O}(1/\sqrt{N})$ synapses, and additional nonlinearities in the single-neuron dynamics.

ACKNOWLEDGEMENTS

We thank Michael A. Buice and Brent Doiron for conversations that shaped the evolution of this manuscript, and Stefano Recanatesi for helpful feedback on a draft version.

Appendix A: Joint probability density functional

We will construct the joint probability density of the membrane potentials and spike trains using the response variable path integral formalism [37–40], reviewed in [109–111]. We will use boldface lowercase variables for vectors and boldface capital letters for matrices/operators. Given the membrane potentials v_{it} , we will require that the spikes generated in the network are conditionally independent across neurons i and time points t . The joint probability density of the membrane potentials \mathbf{v} and the spikes \mathbf{n} , conditioned on the stochastic spike generation, is

$$p(\mathbf{v}, \mathbf{n} | \eta) = \prod_{i=1}^N \prod_{t=1}^{T-1} \delta \left(\frac{dv_{it}}{dt} - E_{it} - \sum_{j,s} J_{ijs} dn_{j,t-s} + \frac{dn_{it}}{dt} v_{it} \right) \times \delta (dn_{it} - \eta_{it}). \quad (\text{A1})$$

Here, $\eta_{it} \sim \text{Bernoulli}(f(v_{it}) dt)$. Introducing the Fourier representation of the delta functions and marginalizing over η yields the joint density

$$p(\mathbf{v}, \mathbf{n}) = \int D\tilde{\mathbf{v}} \int D\tilde{\mathbf{n}} \exp \left(\sum_{i,t} \tilde{v}_{it} \left(\frac{dv_{it}}{dt} - E_{it} - \sum_{j,s} J_{ijs} dn_{j,t-s} + \frac{dn_{it}}{dt} v_{it} \right) - \tilde{n}_{it} dn_{it} + \ln (1 + f(v_{it}) dt (\exp(\tilde{n}_{it}) - 1)) \right). \quad (\text{A2})$$

The measures are $D\tilde{\mathbf{n}} = \prod_{i,t} \frac{d\tilde{n}_{it}}{2\pi i}$ and $D\tilde{\mathbf{v}} = \prod_{i,t} \frac{d\tilde{v}_{it}}{2\pi i}$. The integrals over the response variables, $\tilde{\mathbf{n}}$ and $\tilde{\mathbf{v}}$, are along the imaginary axis. The logarithmic term in the exponent is the cumulant generating function of the Bernoulli spikes. We next take a continuous time limit, $dt \rightarrow 0, T \rightarrow \infty$ with their product fixed. With $dt \ll 1$, we expand the natural logarithm in its Taylor series around 1: $\ln(1 + f(v_{it}) dt (\exp(\tilde{n}_{it}) - 1)) = f(v_{it}) dt (\exp(\tilde{n}_{it}) - 1) + \mathcal{O}((dt)^2)$. This yields Eq. 3.

Appendix B: Microscopic fluctuations in the N -dimensional network

To study fluctuations, we can expand around that mean field theory. We shift \mathbf{v} and $\tilde{\mathbf{n}}$ by their mean field values,

$$\mathbf{v} = \bar{\mathbf{v}} + \delta\mathbf{v}, \quad \tilde{\mathbf{n}} = f(\bar{\mathbf{v}}) + \delta\tilde{\mathbf{n}}, \quad (\text{B1})$$

where $\bar{\mathbf{v}}$ is a solution to Eq. 4. We insert this decomposition into the action $S[\delta\mathbf{v}, \delta\tilde{\mathbf{n}}, \tilde{\mathbf{v}}, \tilde{\mathbf{n}}]$, Eq. 3, expand $(\exp \tilde{n}_i - 1)$, and collect bilinear terms in the response and configuration variables into a free action $S_0[\delta\mathbf{v}, \delta\tilde{\mathbf{n}}, \tilde{\mathbf{v}}, \tilde{\mathbf{n}}]$ so that

$$\begin{aligned} S &= S_0[\delta\mathbf{v}, \delta\tilde{\mathbf{n}}, \tilde{\mathbf{v}}, \tilde{\mathbf{n}}] + S_V[\delta\mathbf{v}, \delta\tilde{\mathbf{n}}, \tilde{\mathbf{v}}, \tilde{\mathbf{n}}] \\ S_0 &= \sum_i \int dt -\tilde{v}_i(t) (\delta_t + 1 + f(\bar{v}_i(t))) \delta v_i(t) - \tilde{v}_i(t) \sum_j \int ds (\delta_{ij} \delta(s) \bar{v}_j(t) - J_{ij}(s)) \delta n_j(t-s) \\ &\quad + \tilde{n}_i(t) \delta n_i(t) - \tilde{n}_i(t) f_i^{(1)} \delta v_i(t) \\ S_V &= \sum_i \int dt -\tilde{v}_i(t) \delta n_i(t) \delta v_i(t) - \sum_{\substack{p,q=1 \\ p+q>2}}^{\infty} \frac{\tilde{n}_i^p f_i^{(q)}}{p! q!} (\delta v_i)^q - f(\bar{v}_i)(t) \sum_{p=2}^{\infty} \frac{\tilde{n}_i^p}{p!}. \end{aligned} \quad (\text{B2})$$

S_0 is the free action; its terms comprise the inverse propagator \mathbf{K} . S_V contains the interacting terms that give rise to vertices in the Feynman diagrams. The model has the same vertices as the Poisson generalized linear model [53], as well as the trilinear coupling $\tilde{v}_i(t)\delta n_i(t)\delta v_i(t)$. Note that at each term in S_V , each of the p factors of \tilde{n}_i and the q factors of δv have their own time variable, each of which is integrated over; we have suppressed these dependencies and integrals for brevity. The trilinear vertex exposes even a neuron with linear hazard function f to loop corrections.

This expansion around the N -dimensional mean field

$$\begin{aligned}
S &= S_0[\delta \mathbf{v}, \delta \mathbf{n}, \tilde{\mathbf{v}}, \tilde{\mathbf{n}}] + S_V[\delta \mathbf{v}, \delta \mathbf{n}, \tilde{\mathbf{v}}, \tilde{\mathbf{n}}], \\
S_0 &= \sum_i \int dt -\tilde{v}_i(t)(\delta_t + 1)\delta v_i(t) - \tilde{v}_i(t) \sum_j \int ds (\delta_{ij}\delta(s)r(s) - J_{ij}(s))\delta n_j(t-s) \\
&\quad + \tilde{n}_i(t)\delta n_i(t) - \tilde{n}_i(t)f_i^{(1)}\delta v_i(t), \\
S_V &= \sum_i \int dt - \sum_{\substack{p,q=1 \\ p+q>2}}^{\infty} \frac{\tilde{n}_i^p f_i^{(q)}}{p! q!} (\delta v_i)^q - f(\tilde{v}_i)(t) \sum_{p=2}^{\infty} \frac{\tilde{n}_i^p}{p!}.
\end{aligned} \tag{B3}$$

This model has the same vertices as the Poisson generalized linear model [53]; the linear hyperpolarization after a spike only affects the mean field theory and the propagator.

2. Feynman rules for the N -dimensional network

Expanding $\exp -S_V$ in its functional Taylor series, any cumulant or moment of $(\delta \dot{\mathbf{n}}, \mathbf{v})$ can be calculated as a series of moments with respect to the free distribution, $\exp -S_0$ via Wick's theorem. These calculations can be summarized in Feynman diagrams. The Feynman rules for the stochastic LIF model are similar to those of the model without spike resets [53], except that 1) there can be propagators linking the response and configuration variables of the spikes and membrane potential and 2) the action of Eq. B2 has the additional trilinear vertex arising from the spike resets. The bare propagators around a fixed point are, in the Fourier domain,

$$\begin{aligned}
\begin{pmatrix} \bar{\Delta}_{\delta n, \tilde{n}} & \bar{\Delta}_{\delta v, \tilde{n}} \\ \bar{\Delta}_{\delta n, \tilde{v}} & \bar{\Delta}_{\delta v, \tilde{v}} \end{pmatrix}(\omega) &= \begin{pmatrix} K_{\delta n, \tilde{n}} & K_{\delta v, \tilde{n}} \\ K_{\delta n, \tilde{v}} & K_{\delta v, \tilde{v}} \end{pmatrix}^{-1}(\omega) \\
&= \begin{pmatrix} \mathbf{I} & -\mathbf{f}'\mathbf{I} \\ -\mathbf{I}\tilde{\mathbf{v}} + \mathbf{J}(\omega) & -i\omega - \mathbf{1} - \mathbf{I}\tilde{\mathbf{f}} \end{pmatrix}^{-1}
\end{aligned} \tag{B4}$$

The interacting action S_V defines the source vertex, $\bar{\mathbf{f}} = \bullet$, as well as the two types of internal vertex. The vertex corresponding to $\tilde{v}_i\delta n_i\delta v_i$ carries a vertex factor of 1. The vertex corresponding to $\frac{\tilde{n}_i^p}{p!} \frac{f_i^{(q)}}{q!} (\delta v_i)^q$ carries

theory allows the systematic study of finite-size networks with a particular connectivity \mathbf{J} , without the requirement of any assumptions on the distribution of connection strengths except that the mean field theory $\bar{\mathbf{v}}$ is stable [85, 112, 113].

1. Microscopic fluctuations in the linear-reset model

Expanding around the mean field theory of Eq. 8 in the action, Eq. 7, we obtain the free and interacting actions:

a vertex factor of $\frac{f_i^{(q)}}{q!}$ [53]. To calculate a joint cumulant density function $\langle\langle \prod_{i=1}^a \dot{n}_i(t_i), \prod_{j=1}^b v_j(s_j) \rangle\rangle$, we can draw all possible connected graphs with a leaf for each of the a factors of $\dot{\mathbf{n}}$ and b factors of \mathbf{v} . For each diagram, each internal vertex has a unique associated neuron index and time variable. We multiply together the vertex factors of the internal vertices and the propagator edges connecting them, sum over all internal neuron indices and integrate over all internal time variables. Finally, we add the contributions of each diagram.

If the mean field rate is at a fixed point, the calculations are simpler in the Fourier domain. Each propagator edge has its own frequency. Each internal vertex is scaled by $(2\pi)^{-q}$, where q is its number of incoming edges. At each internal vertex, momentum is conserved: the sum of all incoming frequencies equals the sum of all outgoing frequencies. Additionally, the frequencies of the external edges sum to 0. To calculate a cumulant, we again draw all connected diagrams. For each diagram, we multiply its vertex factors together, sum over all internal neuron indices, and integrate over the frequencies of each internal edge. Finally, we add the contributions of each diagram.

Appendix C: Mean field theory of homogenous networks

To examine the interaction between synaptic connectivity, subthreshold dynamics and stochastic spike emission in shaping network activity, we will average the partition function for the activity (equivalently, average the

moment generating functional) over the synaptic connectivity. This is a standard exercise in statistical field theory [111]. Let $\langle J_{ij}(s) \rangle_{\mathbf{J}} = J(s)/N$. The average over the connectivity yields:

$$Z = \int \mathcal{D}\mathbf{v} \int \mathcal{D}\tilde{\mathbf{v}} \int \mathcal{D}\mathbf{n} \int \mathcal{D}\tilde{\mathbf{n}} \exp \sum_i \left(\tilde{v}_i^T \left(\dot{v}_i + v_i + \dot{n}_i v_i - E_i - \frac{1}{N} J * \sum_j \dot{n}_j \right) - \tilde{n}_i^T \dot{n}_i + (e^{\tilde{n}_i} - 1)^T f(v_i) \right) \quad (\text{C1})$$

Let $R = \frac{1}{N} \sum_j J * \dot{n}_j$; we will enforce this by integrating against $\delta \left(NR - J * \sum_j \dot{n}_j \right)$. With the Fourier representation of that delta function, we have a generating functional for the auxiliary fields R, \tilde{R} :

$$Z[k, \tilde{k}] = \int \mathcal{D}R \int \mathcal{D}\tilde{R} \exp \left(-N \tilde{R}^T R + \sum_i \ln Z_i[R, \tilde{R}] + k^T R + \tilde{k}^T \tilde{R} \right),$$

$$Z_i[R, \tilde{R}] = \int \mathcal{D}v_i \int \mathcal{D}\tilde{v}_i \int \mathcal{D}n_i \int \mathcal{D}\tilde{n}_i \exp \left(\tilde{v}_i^T (\dot{v}_i + v_i - E - R + \dot{n}_i v_i) + \tilde{R}^T (J * \dot{n}_i) - \tilde{n}_i^T \dot{n}_i + (e^{\tilde{n}_i} - 1)^T f(v_i) \right). \quad (\text{C2})$$

Note that the generating function for the neural dynamics factorizes over the neurons; $Z_i[R, \tilde{R}]$ does not contain any other indices. So, we will drop the neuron indices and write $N \ln Z[R, \tilde{R}]$ instead of $\sum_i \ln Z_i[R, \tilde{R}]$. For large N , we evaluate the integrals over the auxiliary fields R, \tilde{R} by a saddle point approximation. The saddle point equa-

tions are

$$0 = -NR^* + N \frac{\partial \ln Z[R, \tilde{R}]}{\partial \tilde{R}} \Big|_R^* \leftrightarrow R^* = J * \langle \dot{n} \rangle, \quad (\text{C3})$$

$$0 = -N\tilde{R}^* + N \frac{\partial \ln Z[R, \tilde{R}]}{\partial R} \Big|_{\tilde{R}}^* \leftrightarrow \tilde{R}^* = -\langle \tilde{v} \rangle = 0.$$

Here, $\langle \dot{n} \rangle(t)$ is the population-averaged firing rate. Inserting these saddle-point solutions yields the partition function, Eq. 11.

-
- [1] W. J. Freeman, *Mass Action in the Nervous System: Examination of the Neurophysiological Basis of Adaptive Behavior Through the EEG* (Academic Press, 1975) google-Books-ID: D_RqAAAAMAAJ.
 - [2] S. Coombes, *NeuroImage Computational Models of the Brain*, **52**, 731 (2010).
 - [3] P. C. Bressloff, *Journal of Physics A: Mathematical and Theoretical* **45**, 033001 (2011), publisher: IOP Publishing.
 - [4] R. Moran, D. Pinotsis, and K. Friston, *Frontiers in Computational Neuroscience* **7**, 57 (2013).
 - [5] S. Grossberg, *Bulletin of the American Mathematical Society* **75**, 1238 (1969).
 - [6] S.-I. Amari, *Proceedings of the IEEE* **59**, 35 (1971), conference Name: Proceedings of the IEEE.
 - [7] S.-I. Amari, *IEEE Transactions on Systems, Man, and Cybernetics SMC-2*, 643 (1972), conference Name: IEEE Transactions on Systems, Man, and Cybernetics.
 - [8] H. R. Wilson and J. D. Cowan, *Biophysical Journal* **12**, 1 (1972).
 - [9] H. R. Wilson and J. D. Cowan, *Kybernetik* **13**, 55 (1973).
 - [10] T. Ohira and J. D. Cowan, *Physical Review E* **48**, 2259 (1993).
 - [11] I. Ginzburg and H. Sompolinsky, *Physical Review E* **50**, 3171 (1994).
 - [12] M. A. Buice and J. D. Cowan, *Physical Review E* **75**, 051919 (2007).
 - [13] P. C. Bressloff, *SIAM Journal on Applied Mathematics* **70**, 1488 (2010), publisher: Society for Industrial and Applied Mathematics.
 - [14] A. L. Hodgkin and A. F. Huxley, *The Journal of Physiology* **117**, 500 (1952).
 - [15] C. C. Chow and Y. Karimipannah, *Journal of Neurophysiology* **123**, 1645 (2020), publisher: American Physiological Society.
 - [16] N. Brunel, V. Hakim, and M. J. Richardson, *Current Opinion in Neurobiology Theoretical and computational neuroscience*, **25**, 149 (2014).
 - [17] B. Doiron, A. Litwin-Kumar, R. Rosenbaum, G. K.

- Ocker, and K. Josić, *Nature Neuroscience* **19**, 383 (2016).
- [18] B. W. Knight, *Journal of General Physiology* **59**, 734 (1972).
- [19] L. M. Ricciardi, *Diffusion Processes and Related Topics in Biology*, Lecture Notes in Biomathematics, Vol. 14 (Springer Science & Business Media, 1977) google-Books-ID: yyXsCAAQBAJ.
- [20] D. J. Amit and N. Brunel, *Cerebral Cortex* **7**, 237 (1997).
- [21] N. Brunel, *Journal of Computational Neuroscience* **8**, 183 (2000).
- [22] B. Lindner and L. Schimansky-Geier, *Physical Review Letters* **86**, 2934 (2001), publisher: American Physical Society.
- [23] B. Doiron, B. Lindner, A. Longtin, L. Maler, and J. Bastian, *Phys Rev Let* **93** (2004).
- [24] B. Lindner, B. Doiron, and A. Longtin, *Phys. Rev. E* **72** (2005).
- [25] B. Lindner, *Physical Review E* **73**, 022901 (2006), publisher: American Physical Society.
- [26] R. Moreno-Bote and N. Parga, *Physical Review Letters* **96**, 028101 (2006), publisher: American Physical Society.
- [27] T. Schwalger, F. Droste, and B. Lindner, *Journal of Computational Neuroscience* **39**, 29 (2015).
- [28] S. Vellmer and B. Lindner, *Physical Review Research* **1**, 023024 (2019), publisher: American Physical Society.
- [29] W. Gerstner, *Physical Review E* **51**, 738 (1995), publisher: American Physical Society.
- [30] W. Gerstner, *Neural Computation* **12**, 43 (2000).
- [31] C. Meyer and C. v. Vreeswijk, *Neural Computation* **14**, 369 (2002).
- [32] M. Deger, T. Schwalger, R. Naud, and W. Gerstner, *Physical Review E* **90**, 062704 (2014).
- [33] G. Dumont, A. Payeur, and A. Longtin, *PLOS Computational Biology* **13**, e1005691 (2017), publisher: Public Library of Science.
- [34] T. Schwalger, M. Deger, and W. Gerstner, *PLOS Computational Biology* **13**, e1005507 (2017), publisher: Public Library of Science.
- [35] M. Mattia and P. Del Giudice, *Physical Review E* **66**, 051917 (2002).
- [36] B. Pietras, N. Gallice, and T. Schwalger, *Physical Review E* **102**, 022407 (2020), publisher: American Physical Society.
- [37] P. C. Martin, E. D. Siggia, and H. A. Rose, *Physical Review A* **8**, 423 (1973).
- [38] C. D. Dominicis, *Le Journal de Physique Colloques* **37**, C1 (1976).
- [39] H.-K. Janssen, *Zeitschrift für Physik B Condensed Matter* **23**, 377 (1976).
- [40] R. V. Jensen, *Journal of Statistical Physics* **25**, 183 (1981).
- [41] H. Sompolinsky, A. Crisanti, and H. J. Sommers, *Physical Review Letters* **61**, 259 (1988).
- [42] M. Stern, H. Sompolinsky, and L. F. Abbott, *Physical Review E* **90**, 062710 (2014).
- [43] J. Aljadeff, M. Stern, and T. Sharpee, *Physical Review Letters* **114**, 088101 (2015).
- [44] P. C. Bressloff, *The Journal of Mathematical Neuroscience (JMN)* **5**, 4 (2015).
- [45] S. Goedeke, J. Schuecker, and M. Helias, arXiv:1603.01880 [nlin, q-bio] (2016), arXiv: 1603.01880.
- [46] F. Mastrogiuseppe and S. Ostojic, *Neuron* **99**, 609 (2018).
- [47] U. Pereira and N. Brunel, *Neuron* **99**, 227 (2018).
- [48] J. Schuecker, S. Goedeke, and M. Helias, *Physical Review X* **8**, 041029 (2018).
- [49] F. Schuessler, A. Dubreuil, F. Mastrogiuseppe, S. Ostojic, and O. Barak, *Physical Review Research* **2**, 013111 (2020), publisher: American Physical Society.
- [50] I. D. Landau and H. Sompolinsky, *Physical Review Research* **3**, 023171 (2021), publisher: American Physical Society.
- [51] A. van Meegen, T. Kühn, and M. Helias, *Physical Review Letters* **127**, 158302 (2021), publisher: American Physical Society.
- [52] M. A. Buice and C. C. Chow, *PLoS Comput Biol* **9**, e1002872 (2013).
- [53] G. K. Ocker, K. Josić, E. Shea-Brown, and M. A. Buice, *PLOS Computational Biology* **13**, e1005583 (2017).
- [54] B. A. W. Brinkman, F. Rieke, E. Shea-Brown, and M. A. Buice, *PLOS Computational Biology* **14**, e1006490 (2018), publisher: Public Library of Science.
- [55] D. Todorov and W. Truccolo, in *2019 41st Annual International Conference of the IEEE Engineering in Medicine and Biology Society (EMBC)* (2019) pp. 4380–4386, iSSN: 1558-4615.
- [56] M. Kordovan and S. Rotter, arXiv:2001.05057 [physics, q-bio, stat] (2020), arXiv: 2001.05057.
- [57] J. S. Griffith, *Biophysical Journal* **3**, 299 (1963).
- [58] M. V. Tsodyks, W. E. Skaggs, T. J. Sejnowski, and B. L. McNaughton, *The Journal of Neuroscience* **17**, 4382 (1997).
- [59] H. Ozeki, I. M. Finn, E. S. Schaffer, K. D. Miller, and D. Ferster, *Neuron* **62**, 578 (2009), publisher: Elsevier.
- [60] H. K. Kato, S. K. Asinof, and J. S. Isaacson, *Neuron* **95**, 412 (2017), publisher: Elsevier.
- [61] H. Adesnik, *Neuron* **95**, 1147 (2017), publisher: Elsevier.
- [62] A. Sanzeni, B. Akitake, H. C. Goldbach, C. E. Leedy, N. Brunel, and M. H. Histed, *eLife* **9**, e54875 (2020), publisher: eLife Sciences Publications, Ltd.
- [63] D. Cox and V. Isham, *Point Processes*, Monographs on Statistics and Applied Probability (CRC Press, 1980).
- [64] Z. Zhou, Y. Zhang, Y. Xie, Z. Wang, and J.-G. Liu, *Mathematical Neuroscience and Applications Volume 1* (2021), 10.46298/mna.7203, publisher: Epi-science.org.
- [65] W. Gerstner, W. M. Kistler, R. Naud, and L. Paninski, *Neuronal Dynamics: From Single Neurons to Networks and Models of Cognition* (Cambridge University Press, 2014) google-Books-ID: D4j2AwAAQBAJ.
- [66] K. D. Miller and T. W. Troyer, *J Neurophysiol.* **87**, 653 (2002).
- [67] D. Hansel and C. v. Vreeswijk, *Journal of Neuroscience* **22**, 5118 (2002), publisher: Society for Neuroscience Section: ARTICLE.
- [68] N. J. Priebe, F. Mechler, M. Carandini, and D. Ferster, *Nature Neuroscience* **7**, 1113 (2004).
- [69] N. J. Priebe and D. Ferster, *Nature Neuroscience* **9**, 552 (2006).
- [70] D. Linaro, G. K. Ocker, B. Doiron, and M. Giugliano, *Journal of Neuroscience* **39**, 7648 (2019).
- [71] W. Gerstner and J. L. v. Hemmen, *Biological Cybernetics* **67**, 195 (1992).

- [72] P. Robert and J. Touboul, *Journal of Statistical Physics* **165**, 545 (2016).
- [73] B. Rudy, G. Fishell, S. Lee, and J. Hjerling-Leffler, *Developmental Neurobiology* **71**, 45 (2011).
- [74] B. Tasic, V. Menon, T. N. Nguyen, T. K. Kim, T. Jarsky, Z. Yao, B. Levi, L. T. Gray, S. A. Sorensen, T. Dolbeare, D. Bertagnolli, J. Goldy, N. Shapovalova, S. Parry, C. Lee, K. Smith, A. Bernard, L. Madisen, S. M. Sunkin, M. Hawrylycz, C. Koch, and H. Zeng, *Nature Neuroscience* **19**, 335 (2016).
- [75] Z. Yao, C. T. J. v. Velthoven, T. N. Nguyen, J. Goldy, A. E. Seden-Cortes, F. Baftizadeh, D. Bertagnolli, T. Casper, M. Chiang, K. Crichton, S.-L. Ding, O. Fong, E. Garren, A. Glandon, N. W. Gouwens, J. Gray, L. T. Graybuck, M. J. Hawrylycz, D. Hirschstein, M. Kroll, K. Lathia, C. Lee, B. Levi, D. McMillen, S. Mok, T. Pham, Q. Ren, C. Rimorin, N. Shapovalova, J. Sulc, S. M. Sunkin, M. Tieu, A. Torkelson, H. Tung, K. Ward, N. Dee, K. A. Smith, B. Tasic, and H. Zeng, *Cell* **184**, 3222 (2021), publisher: Elsevier.
- [76] E. M. Callaway, H.-W. Dong, J. R. Ecker, M. J. Hawrylycz, Z. J. Huang, E. S. Lein, J. Ngai, P. Osten, B. Ren, A. S. Tolias, O. White, H. Zeng, X. Zhuang, G. A. Ascoli, M. M. Behrens, J. Chun, G. Feng, J. C. Gee, S. S. Ghosh, Y. O. Halchenko, R. Hertzano, B. K. Lim, M. E. Martone, L. Ng, L. Pachter, A. J. Ropelewski, T. L. Tickle, X. W. Yang, K. Zhang, T. E. Bakken, P. Berens, T. L. Daigle, J. A. Harris, N. L. Jorstad, B. E. Kalmbach, D. Kobak, Y. E. Li, H. Liu, K. S. Matho, E. A. Mukamel, M. Naeemi, F. Scala, P. Tan, J. T. Ting, F. Xie, M. Zhang, Z. Zhang, J. Zhou, B. Zingg, E. Armand, Z. Yao, D. Bertagnolli, T. Casper, K. Crichton, N. Dee, D. Diep, S.-L. Ding, W. Dong, E. L. Dougherty, O. Fong, M. Goldman, J. Goldy, R. D. Hodge, L. Hu, C. D. Keene, F. M. Krienen, M. Kroll, B. B. Lake, K. Lathia, S. Linnarsson, C. S. Liu, E. Z. Macosko, S. A. McCarroll, D. McMillen, N. M. Nadaf, T. N. Nguyen, C. R. Palmer, T. Pham, N. Plongthongkum, N. M. Reed, A. Regev, C. Rimorin, W. J. Romanow, S. Savoia, K. Siletti, K. Smith, J. Sulc, B. Tasic, M. Tieu, A. Torkelson, H. Tung, C. T. J. van Velthoven, C. R. Vanderburg, A. M. Yanny, R. Fang, X. Hou, J. D. Lucero, J. K. Osteen, A. Pinto-Duarte, O. Poirion, S. Preissl, X. Wang, A. I. Aldridge, A. Bartlett, L. Boggeman, C. O'Connor, R. G. Castanon, H. Chen, C. Fitzpatrick, C. Luo, J. R. Nery, M. Nunn, A. C. Rivkin, W. Tian, B. Dominguez, T. Ito-Cole, M. Jacobs, X. Jin, C.-T. Lee, K.-F. Lee, P. A. Miyazaki, Y. Pang, M. Rashid, J. B. Smith, M. Vu, E. Williams, T. Biancalani, A. S. Boeshaghi, M. Crow, S. Dudoit, S. Fischer, J. Gillis, Q. Hu, P. V. Kharchenko, S.-Y. Niu, V. Ntranos, E. Purdom, D. Risso, H. R. de Bézieux, S. Somasundaram, K. Street, V. Svensson, E. D. Vaishnav, K. Van den Berge, J. D. Welch, X. An, H. S. Bateup, I. Bowman, R. K. Chance, N. N. Foster, W. Galbavy, H. Gong, L. Gou, J. T. Hatfield, H. Hintiryan, K. E. Hirokawa, G. Kim, D. J. Kramer, A. Li, X. Li, Q. Luo, R. Muñoz-Castañeda, D. A. Stafford, Z. Feng, X. Jia, S. Jiang, T. Jiang, X. Kuang, R. Larsen, P. Lesnar, Y. Li, Y. Li, L. Liu, H. Peng, L. Qu, M. Ren, Z. Ruan, E. Shen, Y. Song, W. Wakeman, P. Wang, Y. Wang, Y. Wang, L. Yin, J. Yuan, S. Zhao, X. Zhao, A. Narasimhan, R. Palaniswamy, S. Banerjee, L. Ding, D. Huilgol, B. Huo, H.-C. Kuo, S. Latusnus, X. Li, P. P. Mitra, J. Mizrachi, Q. Wang, P. Xie, F. Xiong, Y. Yu, S. W. Eichhorn, J. Berg, M. Bernabucci, Y. Bernaerts, C. R. Cadwell, J. R. Castro, R. Dalley, L. Hartmanis, G. D. Horwitz, X. Jiang, A. L. Ko, E. Miranda, S. Mulherkar, P. R. Nicovich, S. F. Owen, R. Sandberg, S. A. Sorensen, Z. H. Tan, S. Allen, D. Hockemeyer, A. Y. Lee, M. B. Veldman, R. S. Adkins, S. A. Ament, H. C. Bravo, R. Carter, A. Chatterjee, C. Colantuoni, J. Crabtree, H. Creasy, V. Felix, M. Giglio, B. R. Herb, J. Kancherla, A. Mahurkar, C. McCracken, L. Nickel, D. Olley, J. Orvis, M. Schor, G. Hood, B. Dichter, M. Grauer, B. Helba, A. Bandrowski, N. Barkas, B. Carlin, F. D. D'Orazi, K. Degatano, T. H. Gillespie, F. Khajouei, K. Konwar, C. Thompson, K. Kelly, S. Mok, S. Sunkin, BRAIN Initiative Cell Census Network (BICCN), BRAIN Initiative Cell Census Network (BICCN) Corresponding authors, BICCN contributing principal investigators, Principal manuscript editors, Manuscript writing and figure generation, Analysis coordination, Integrated data analysis, scRNA-seq and snRNA-seq data generation and processing, ATAC-seq data generation and processing, Methylcytosine data production and analysis, Epi-retro-seq data generation and processing, 'Omics data analysis, Tracing and connectivity data generation, Morphology data generation and reconstruction, OLST/STPT and other data generation, c. a. i. a. Morphology, Spatially resolved single-cell transcriptomics (MERFISH), Multimodal profiling (Patch-seq), Transgenic tools, NeMO archive and analytics, Brain Image Library (BIL) archive, DANDI archive, Brain Cell Data Center (BCDC), and Project management, *Nature* **598**, 86 (2021), number: 7879 Publisher: Nature Publishing Group.
- [77] C. K. Pfeffer, M. Xue, M. He, Z. J. Huang, and M. Scanziani, *Nature Neuroscience* **16**, 1068 (2013), bandiera_abtest: a Cg-type: Nature Research Journals Number: 8 Primary_atype: Research Publisher: Nature Publishing Group Subject_term: Inhibition;Molecular neuroscience;Visual system Subject_term_id: inhibition;molecular-neuroscience;visual-system.
- [78] R. Tremblay, S. Lee, and B. Rudy, *Neuron* **91**, 260 (2016).
- [79] S. C. Seeman, L. Campagnola, P. A. Davoudian, A. Hoggarth, T. A. Hage, A. Bosma-Moody, C. A. Baker, J. H. Lee, S. Mihalas, C. Teeter, A. L. Ko, J. G. Ojemann, R. P. Gwinn, D. L. Silbergeld, C. Cobbs, J. Phillips, E. Lein, G. Murphy, C. Koch, H. Zeng, and T. Jarsky, *eLife* (2018), 10.7554/eLife.37349.
- [80] T. A. Hage, A. Bosma-Moody, C. A. Baker, M. B. Kratz, L. Campagnola, T. Jarsky, H. Zeng, and G. J. Murphy, *eLife* **11**, e71103 (2022), publisher: eLife Sciences Publications, Ltd.
- [81] A. Litwin-Kumar, R. Rosenbaum, and B. Doiron, *Journal of Neurophysiology* **115**, 1399 (2016).
- [82] A. Kohn, R. Coen-Cagli, I. Kanitscheider, and A. Pouget, *Annual Review of Neuroscience* **39**, 237 (2016).
- [83] R. Kempter, W. Gerstner, and J. L. Van Hemmen, *Physical Review E* **59**, 4498 (1999).
- [84] M. Gilson, A. Burkitt, and J. L. v. Hemmen, *Frontiers in Computational Neuroscience* **4**, 23 (2010).
- [85] G. K. Ocker, A. Litwin-Kumar, and B. Doiron, *PLoS Comput Biol* **11**, e1004458 (2015).

- [86] N. R. Tannenbaum and Y. Burak, PLOS Comput Biol **12**, e1005056 (2016).
- [87] G. K. Ocker and B. Doiron, Cerebral Cortex (2018), 10.1093/cercor/bhy001.
- [88] L. Montangie, C. Miehl, and J. Gjorgjieva, PLOS Computational Biology **16**, e1007835 (2020), publisher: Public Library of Science.
- [89] D. R. Cox, *Renewal Theory* (Methuen, 1962) google-Books-ID: 0VxRAAAAMAAJ.
- [90] F. Randi and A. M. Leifer, Physical Review Letters **126**, 118102 (2021), publisher: American Physical Society.
- [91] T. Ohyama, C. M. Schneider-Mizell, R. D. Fetter, J. V. Aleman, R. Franconville, M. Rivera-Alba, B. D. Mensh, K. M. Branson, J. H. Simpson, J. W. Truman, A. Cardona, and M. Zlatic, Nature **520**, 633 (2015).
- [92] M. E. Berck, A. Khandelwal, L. Claus, L. Hernandez-Nunez, G. Si, C. J. Tabone, F. Li, J. W. Truman, R. D. Fetter, M. Louis, A. D. Samuel, and A. Cardona, eLife (2016), 10.7554/eLife.14859.
- [93] A. A. Wanner, C. Genoud, T. Masudi, L. Siksou, and R. W. Friedrich, Nature Neuroscience **19**, 816 (2016), bandiera_abtest: a Cg.type: Nature Research Journals Number: 6 Primary_atype: Research Publisher: Nature Publishing Group Subject.term: Neural circuits;Olfactory bulb;Scanning electron microscopy Subject_term_id: neural-circuit;olfactory-bulb;scanning-electron-microscopy.
- [94] J. L. Morgan, D. R. Berger, A. W. Wetzels, and J. W. Lichtman, Cell **165**, 192 (2016).
- [95] I. Larderet, P. M. Fritsch, N. Gendre, G. L. Neagu-Maier, R. D. Fetter, C. M. Schneider-Mizell, J. W. Truman, M. Zlatic, A. Cardona, and S. G. Sprecher, eLife **6**, e28387 (2017).
- [96] D. G. C. Hildebrand, M. Cicconet, R. M. Torres, W. Choi, T. M. Quan, J. Moon, A. W. Wetzels, A. S. Champion, B. J. Graham, O. Randlett, G. S. Plummer, R. Portugues, I. H. Bianco, S. Saalfeld, A. D. Baden, K. Lillaney, R. Burns, J. T. Vogelstein, A. F. Schier, W.-C. A. Lee, W.-K. Jeong, J. W. Lichtman, and F. Engert, Nature **545**, 345 (2017).
- [97] K. Eichler, F. Li, A. Litwin-Kumar, Y. Park, I. Andrade, C. M. Schneider-Mizell, T. Saumweber, A. Huser, C. Eschbach, B. Gerber, R. D. Fetter, J. W. Truman, C. E. Priebe, L. F. Abbott, A. S. Thum, M. Zlatic, and A. Cardona, Nature **548**, 175 (2017).
- [98] Z. Zheng, J. S. Lauritzen, E. Perlman, C. G. Robinson, M. Nichols, D. Milkie, O. Torrens, J. Price, C. B. Fisher, N. Sharifi, S. A. Calle-Schuler, L. Kme-cova, I. J. Ali, B. Karsh, E. T. Trautman, J. A. Bogovic, P. Hanslovsky, G. S. X. E. Jefferis, M. Kazhdan, K. Khairy, S. Saalfeld, R. D. Fetter, and D. D. Bock, Cell **0** (2018), 10.1016/j.cell.2018.06.019.
- [99] A. Motta, M. Berning, K. M. Boergens, B. Staffler, M. Beining, S. Loomba, C. Schramm, P. Hennig, H. Wissler, and M. Helmstaedter, bioRxiv , 460618 (2018).
- [100] S. J. Cook, T. A. Jarrell, C. A. Brittin, Y. Wang, A. E. Bloniarz, M. A. Yakovlev, K. C. Q. Nguyen, L. T.-H. Tang, E. A. Bayer, J. S. Duerr, H. E. Bülow, O. Hobert, D. H. Hall, and S. W. Emmons, Nature **571**, 63 (2019), bandiera_abtest: a Cg.type: Nature Research Journals Number: 7763 Primary_atype: Research Publisher: Nature Publishing Group Subject.term: Network models;Neural circuits;Sexual dimorphism Subject_term_id: network-models;neural-circuit;sexual-dimorphism.
- [101] C. S. Xu, M. Januszewski, Z. Lu, S.-y. Takemura, K. J. Hayworth, G. Huang, K. Shinomiya, J. Maitin-Shepard, D. Ackerman, S. Berg, T. Blakely, J. Bogovic, J. Clements, T. Dolafi, P. Hubbard, D. Kainmueller, W. Katz, T. Kawase, K. A. Khairy, L. Leavitt, P. H. Li, L. Lindsey, N. Neubarth, D. J. Olbris, H. Ot-suna, E. T. Troutman, L. Umayam, T. Zhao, M. Ito, J. Goldammer, T. Wolff, R. Svirskas, P. Schlegel, E. R. Neace, C. J. Knecht, C. X. Alvarado, D. A. Bailey, S. Ballinger, J. A. Borycz, B. S. Canino, N. Cheatham, M. Cook, M. Dreher, O. Duclos, B. Eubanks, K. Fairbanks, S. Finley, N. Forknall, A. Francis, G. P. Hopkins, E. M. Joyce, S. Kim, N. A. Kirk, J. Kovalyak, S. A. Lauchie, A. Lohff, C. Maldonado, E. A. Manley, S. McLin, C. Mooney, M. Ndama, O. Ogundeyi, N. Okeoma, C. Ordish, N. Padilla, C. Patrick, T. Paterson, E. E. Phillips, E. M. Phillips, N. Rampally, C. Ribeiro, M. K. Robertson, J. T. Rymer, S. M. Ryan, M. Sammons, A. K. Scott, A. L. Scott, A. Shinomiya, C. Smith, K. Smith, N. L. Smith, M. A. Sobeski, A. Suleiman, J. Swift, S. Takemura, I. Talebi, D. Tarnogorska, E. Tenshaw, T. Tokhi, J. J. Walsh, T. Yang, J. A. Horne, F. Li, R. Parekh, P. K. Rivlin, V. Jayaraman, K. Ito, S. Saalfeld, R. George, I. Meinertzhagen, G. M. Rubin, H. F. Hess, L. K. Scheffer, V. Jain, and S. M. Plaza, bioRxiv , 2020.01.21.911859 (2020), publisher: Cold Spring Harbor Laboratory Section: New Results.
- [102] M. Consortium, J. A. Bae, M. Baptiste, A. L. Bodor, D. Brittain, J. Buchanan, D. J. Bumbarger, M. A. Castro, B. Celii, E. Cobos, F. Collman, N. M. d. Costa, S. Dorcenwald, L. Elabbady, P. G. Fahey, T. Fliss, E. Froudarakis, J. Gager, C. Gamlin, A. Halageri, J. Hebditch, Z. Jia, C. Jordan, D. Kapner, N. Kemnitz, S. Kinn, S. Koolman, K. Kuehner, K. Lee, K. Li, R. Lu, T. Macrina, G. Mahalingam, S. McReynolds, E. Miranda, E. Mitchell, S. S. Mondal, M. Moore, S. Mu, T. Muhammad, B. Nehoran, O. Ogedengbe, C. Papadopoulos, S. Papadopoulos, S. Patel, X. Pitkow, S. Popovych, A. Ramos, R. C. Reid, J. Reimer, C. M. Schneider-Mizell, H. S. Seung, B. Silverman, W. Silversmith, A. Sterling, F. H. Sinz, C. L. Smith, S. Suckow, M. Takeno, Z. H. Tan, A. S. Tolia, R. Torres, N. L. Turner, E. Y. Walker, T. Wang, G. Williams, S. Williams, K. Willie, R. Willie, W. Wong, J. Wu, C. Xu, R. Yang, D. Yatsenko, F. Ye, W. Yin, and S.-c. Yu, *Functional connectomics spanning multiple areas of mouse visual cortex*, Tech. Rep. (2021) company: Cold Spring Harbor Laboratory Distributor: Cold Spring Harbor Laboratory Label: Cold Spring Harbor Laboratory Section: New Results Type: article.
- [103] A. Vishwanathan, A. D. Ramirez, J. Wu, A. Sood, R. Yang, N. Kemnitz, D. Ih, N. Turner, K. Lee, I. Tartavull, W. M. Silversmith, C. S. Jordan, C. David, D. Bland, M. S. Goldman, E. R. F. Aksay, H. S. Seung, and T. Eyewirers, *Predicting modular functions and neural coding of behavior from a synaptic wiring diagram*, Tech. Rep. (2021) company: Cold Spring Harbor Laboratory Distributor: Cold Spring Harbor Laboratory Label: Cold Spring Harbor Laboratory Section: New Results Type: article.
- [104] A. De Masi, A. Galves, E. Löcherbach, and E. Presutti, Journal of Statistical Physics **158**, 866 (2015).

- [105] V. Schmutz, E. Löcherbach, and T. Schwalger, (2021).
- [106] N. Fournier and E. Löcherbach, *Annales de l'Institut Henri Poincaré, Probabilités et Statistiques* **52**, 1844 (2016), publisher: Institut Henri Poincaré.
- [107] A. Duarte and G. Ost, arXiv:1410.6086 [math, q-bio] (2016), arXiv: 1410.6086.
- [108] Q. Cormier, E. Tanré, and R. Veltz, *Stochastic Processes and their Applications* **130**, 2553 (2020), arXiv: 1810.08562.
- [109] C. C. Chow and M. A. Buice, *The Journal of Mathematical Neuroscience (JMN)* **5**, 1 (2015).
- [110] J. A. Hertz, Y. Roudi, and P. Sollich, *Journal of Physics A: Mathematical and Theoretical* **50**, 033001 (2016), publisher: IOP Publishing.
- [111] M. Helias and D. Dahmen, *Statistical Field Theory for Neural Networks*, Lecture Notes in Physics (Springer International Publishing, 2020).
- [112] S. Ostojic, N. Brunel, and V. Hakim, *J Neurosci* **29**, 10234 (2009).
- [113] J. Trousdale, Y. Hu, E. Shea-Brown, and K. Josić, *PLoS Computational Biology* **8**, e1002408 (2012).